

# Convergence of Newton-MR under Inexact Hessian Information

Yang Liu\*      Fred Roosta†

July 13, 2020

## Abstract

Recently, there has been a surge of interest in designing variants of the classical Newton-CG in which the Hessian of a (strongly) convex function is replaced by suitable approximations. This is mainly motivated by large-scale finite-sum minimization problems that arise in many machine learning applications. Going beyond convexity, inexact Hessian information has also been recently considered in the context of algorithms such as trust-region or (adaptive) cubic regularization for general non-convex problems. Here, we do that for Newton-MR, which extends the application range of the classical Newton-CG beyond convexity to invex problems. Unlike the convergence analysis of Newton-CG, which relies on spectrum preserving Hessian approximations in the sense of Löwner partial order, our work here draws from matrix perturbation theory to estimate the distance between the subspaces underlying the exact and approximate Hessian matrices. Numerical experiments demonstrate a great degree of resilience to such Hessian approximations, amounting to a highly efficient algorithm in large-scale problems.

## 1 Introduction

Consider the unconstrained optimization problem:

$$\min_{\mathbf{x} \in \mathbb{R}^d} f(\mathbf{x}), \quad (1)$$

where  $f : \mathbb{R}^d \rightarrow \mathbb{R}$ . Due to simplicity and solid theoretical foundations, there is an abundance of algorithms designed specifically for the case where  $f$  is convex [6, 9, 47]. Strong-convexity, as a special case, allows for the design of algorithms with a great many theoretical and algorithmic properties. In such settings, the classical Newton’s method and its Newton-CG variant hold a special place. In particular, for strongly-convex functions with sufficient degree of smoothness, they have been shown to enjoy various desirable properties including insensitivity to problem ill-conditioning [55, 69], problem-independent local convergence rates [55], and robustness to hyper-parameter tuning [4, 40].

Arguably, the only drawback of Newton’s method in large-scale problems is the computational cost of applying the Hessian matrix. For example, consider the canonical problem of finite-sum minimization where

$$f(\mathbf{x}) = \frac{1}{n} \sum_{i=1}^n f_i(\mathbf{x}), \quad (2)$$

and each  $f_i$  corresponds to an observation (or a measurement), which models the loss (or misfit) given a particular choice of the underlying parameter  $\mathbf{x}$ . Problems of the form (2) arise very often

---

\*School of Mathematics and Physics, University of Queensland, Australia. Email: yang.liu2@uq.edu.au

†School of Mathematics and Physics, University of Queensland, Australia, and International Computer Science Institute, Berkeley, USA. Email: fred.roosta@uq.edu.au

in machine learning, e.g., [60], as well as scientific computing, e.g., [56]. Here, the Hessian matrix can be written as  $\mathbf{H}(\mathbf{x}) = \sum_{i=1}^n \nabla^2 f_i(\mathbf{x})/n$ . In big-data regime where  $n \gg 1$ , operations with the Hessian of  $f$ , e.g., matrix-vector products, typically constitute the main bottleneck of computations. In this light, several recent efforts have focused on the design and analysis of variants of Newton’s method in which the exact Hessian matrix,  $\mathbf{H}(\mathbf{x}) \triangleq \nabla^2 f(\mathbf{x})$  is replaced with its suitable approximation  $\tilde{\mathbf{H}}(\mathbf{x}) \approx \nabla^2 f(\mathbf{x})$ . One such approximation strategy is randomized sub-sampling in which by considering a sample of size  $|\mathcal{S}| \ll n$ , we can form the sub-sampled Hessian as  $\hat{\mathbf{H}}(\mathbf{x}) = \sum_{j \in \mathcal{S}} \nabla^2 f_j(\mathbf{x})/|\mathcal{S}|$ . Under certain conditions, sub-sampling Hessian has been shown to be very effective in reducing the overall computational costs, e.g., [8, 10, 11, 29, 55]. In certain special cases, the structure of  $f$  could also be used for more sophisticated randomized matrix approximation strategies such as sketching and those based on statistical leverage scores, e.g., [53, 69].

However, in the absence of either sufficient smoothness or strong-convexity, the classical Newton’s method and its Newton-CG can simply break down, e.g., their underlying sub-problems may fail to have a solution. Hence, many Newton-type variants have been proposed which aim at extending Newton’s method beyond strongly-convex problems, e.g., Levenberg-Marquardt [42, 43], trust-region [23], cubic regularization [17, 18, 48], and various other methods, which make clever use of negative curvature when it arises [15, 16, 57, 58]. Variants of these methods using inexact function approximations, including approximate Hessian, have also been studied, e.g., [2, 7, 19, 20, 34, 41, 61, 67, 68, 70]. However, many of these methods rely on strict smoothness assumptions such as Lipschitz continuity of gradient and Hessian. In addition, in sharp contrast to Newton’s method whose sub-problems are simple linear systems, a vast majority of these methods involve sub-problems that are themselves non-trivial to solve, e.g., the sub-problems of trust-region and cubic regularization methods are non-linear and non-convex.

To extend the application range of the classical Newton’s method beyond strongly-convex settings, while maintaining the simplicity of its sub-problems, Newton-MR [54] has recently been proposed. Iterations of Newton-MR, at a high level, can be written as  $\mathbf{x}_{k+1} = \mathbf{x}_k - \alpha_k [\mathbf{H}_k]^\dagger \mathbf{g}_k$ , where  $\alpha_k$  is some suitably chosen step-size and  $[\mathbf{H}_k]^\dagger$  is the Moore-Penrose generalized inverse of  $\mathbf{H}_k$ . On the surface, Newton-MR bares a striking resemblance to the classical Newton’s method and shares several of its desirable properties, e.g., Newton-MR involves simple sub-problems in the form of ordinary least squares. However, not only does Newton-MR requires more relaxed smoothness assumptions compared with most non-convex Newton-type methods, but also it can be readily applied to a class of non-convex problems known as *invex* [3, 46], which subsumes convexity as a sub-class. Recall that the class of invex functions, first studied in [37], extends the sufficiency of the first order optimality condition to a broader class of problems than simple convex programming. In other words, the necessary and sufficient condition for any minimizer of invex problem (1) is  $\nabla f(\mathbf{x}^*) = 0$ . However, this is alternatively equivalent to having  $\|\nabla f(\mathbf{x}^*)\| = 0$ , which in turn give rise to the following auxiliary non-convex optimization problem

$$\min_{\mathbf{x} \in \mathbb{R}^d} \frac{1}{2} \|\nabla f(\mathbf{x})\|^2. \quad (3)$$

Since the global minimizers of (3) are the stationary points of (1), when  $f$  is invex, the global minimizers of (1) and (3) coincide. Newton-MR is built upon considering (3), which in turn makes it suitable for (1) with invex objectives. For more general non-convex functions, instead of minimizing  $f$ , the iterations of Newton-MR converge towards the zeros of its gradient field, which are used in many applications, e.g., exploring the loss landscape in chemical physics [1, 66] and deep neural networks [31]. Motivated by the potential and advantages of Newton-MR, in this paper we provide its convergence analysis under inexact Hessian information. In this light, we show that appropriately approximating the Hessian matrix allows for efficient application of Newton-MR to large-scale problems. Before delving any deeper, we note that, while the main motivating class of problems for our work here is that of finite-sum minimization (2), we develop our theory more generally for (1). This is so since for more general objectives, it is also often possible to approximate the Hessian using quasi-Newton methods, e.g., symmetric rank one update [12, 17, 24], or finite-difference approximations [26, 49].

The rest of this paper is organized as follows. We end this section by introducing the notation

and the assumptions on  $f$  used in this paper. In Section 2, we study inexact Hessian information in light of matrix perturbation theory and establish conditions under which such perturbations satisfy a notion of stability. In Section 3, we leverage this stability analysis and provide convergence results for Newton-MR with Hessian approximations. Numerical experiments are presented in Section 4. Conclusions are gathered in Section 5.

## 1.1 Notation

Throughout the paper, vectors and matrices are denoted by bold lower-case and bold upper-case letters, respectively, e.g.,  $\mathbf{v}$  and  $\mathbf{V}$ . We use regular lower-case and upper-case letters to denote scalar constants, e.g.,  $d$  or  $L$ . For a real vector,  $\mathbf{v}$ , its transpose is denoted by  $\mathbf{v}^\top$ . For two vectors  $\mathbf{v}, \mathbf{w}$ , their inner-product is denoted as  $\langle \mathbf{v}, \mathbf{w} \rangle = \mathbf{v}^\top \mathbf{w}$ . For a vector  $\mathbf{v}$  and a matrix  $\mathbf{V}$ ,  $\|\mathbf{v}\|$  and  $\|\mathbf{V}\|$  denote vector  $\ell_2$  norm and matrix spectral norm, respectively. Iteration counter for the main algorithm appears as subscript, e.g.,  $\mathbf{p}_k$ . Iteration counter for sub-problem solver to obtain  $\mathbf{p}_k$  appears as superscript, e.g.,  $\mathbf{p}_k^{(t)}$ . The vector of all zero components is denoted by  $\mathbf{0}$ . For two symmetric matrices  $\mathbf{A}$  and  $\mathbf{B}$ , the Löwner partial order  $\mathbf{A} \succeq \mathbf{B}$  indicates that  $\mathbf{A} - \mathbf{B}$  is symmetric positive semi-definite. For any  $\mathbf{x}, \mathbf{z} \in \mathbb{R}^2$ ,  $\mathbf{y} \in [\mathbf{x}, \mathbf{z}]$  denotes  $\mathbf{y} = \mathbf{x} + \tau(\mathbf{z} - \mathbf{x})$  for some  $0 \leq \tau \leq 1$ .  $\mathbf{A}^\dagger$  denotes the Moore-Penrose generalized inverse of matrix  $\mathbf{A}$ . The element of a matrix  $\mathbf{A}$  located at the  $i^{\text{th}}$  row and the  $j^{\text{th}}$  column is denoted by  $[\mathbf{A}]_{ij}$ .  $\sigma_i(\mathbf{A})$  denotes  $i^{\text{th}}$  largest singular values of a matrix  $\mathbf{A}$ . The eigenvalues of a symmetric matrix  $\mathbf{A} \in \mathbb{R}^{d \times d}$  are ordered as  $\lambda_1(\mathbf{A}) \geq \lambda_2(\mathbf{A}) \geq \dots \lambda_d(\mathbf{A})$ . For simplicity, we use  $\mathbf{g}(\mathbf{x}) \triangleq \nabla f(\mathbf{x}) \in \mathbb{R}^d$  and  $\mathbf{H}(\mathbf{x}) \triangleq \nabla^2 f(\mathbf{x}) \in \mathbb{R}^{d \times d}$  for the gradient and the Hessian of  $f$  at  $\mathbf{x}$ , respectively, and at times we drop the dependence on  $\mathbf{x}$  by simply using  $\mathbf{g}$  and  $\mathbf{H}$ , e.g.,  $\mathbf{g}_k = \mathbf{g}(\mathbf{x}_k)$  and  $\mathbf{H}_k = \mathbf{H}(\mathbf{x}_k)$ . Finally, ‘‘Arg min’’ implies that the minimum may be attained at more than one point.

## 1.2 Assumptions on the Objective Function

Here, we introduce the assumptions on  $f$  in (1) that underlie our work. We note that these assumptions are essentially the same as those in [54].

**Assumption 1** (Differentiability). *The function  $f$  is twice-differentiable.*

In particular, all the first partial derivatives are themselves differentiable, but the second partial derivatives are allowed to be discontinuous. Recall that requiring the first partials be differentiable implies the equality of crossed-partial, which amounts to the symmetric Hessian matrix [38, pp. 732-733].

Instead of the typical smoothness assumptions in the form of Lipschitz continuity of gradient and Hessian, i.e., for some  $0 \leq L_{\mathbf{g}} < \infty$  and  $0 \leq L_{\mathbf{H}} < \infty$

$$\|\mathbf{g}(\mathbf{x}) - \mathbf{g}(\mathbf{y})\| \leq L_{\mathbf{g}} \|\mathbf{x} - \mathbf{y}\|, \quad (4a)$$

$$\|\mathbf{H}(\mathbf{x}) - \mathbf{H}(\mathbf{y})\| \leq L_{\mathbf{H}} \|\mathbf{x} - \mathbf{y}\|, \quad (4b)$$

a more relaxed notion, called moral-smoothness, was introduced in [54].

**Assumption 2** (Moral-smoothness). *For any  $\mathbf{x}_0 \in \mathbb{R}^d$ , there is a constant  $0 < L(\mathbf{x}_0) < \infty$ , such that*

$$\|\mathbf{H}(\mathbf{y})\mathbf{g}(\mathbf{y}) - \mathbf{H}(\mathbf{x})\mathbf{g}(\mathbf{x})\| \leq L(\mathbf{x}_0) \|\mathbf{y} - \mathbf{x}\|, \quad \forall (\mathbf{x}, \mathbf{y}) \in \mathcal{X}_0 \times \mathbb{R}^d, \quad (5)$$

where  $\mathcal{X}_0 \triangleq \{\mathbf{x} \in \mathbb{R}^d \mid \|\mathbf{g}(\mathbf{x})\| \leq \|\mathbf{g}(\mathbf{x}_0)\|\}$ .

Assumption 2 is similar to Lipschitz continuity assumption for the gradient of the auxiliary objective (3), albeit restricted to  $\mathcal{X}_0 \times \mathbb{R}^d$  and with the constant  $L(\mathbf{x}_0)$  that depends on the choice of  $\mathbf{x}_0$ . By (5), it is only the action of Hessian on the gradient that is required to be Lipschitz continuous, and each gradient and/or Hessian individually can be highly irregular, e.g., gradient can be very non-smooth and Hessian can even be discontinuous. In [54], it has been shown that Assumption 2 is significantly more relaxed than (4), i.e., Assumption 2 is implied by (4) and the converse is not true.

**Assumption 3** (Pseudo-inverse Regularity). *There exists a constant  $\gamma > 0$ , such that*

$$\|\mathbf{H}(\mathbf{x})\mathbf{p}\| \geq \gamma \|\mathbf{p}\|, \quad \forall \mathbf{p} \in \text{Range}(\mathbf{H}(\mathbf{x})). \quad (6)$$

Intuitively,  $\gamma$  is a uniform lower-bound on the smallest, in magnitude, among the non-zero eigenvalues of  $\mathbf{H}(\mathbf{x})$ , for any  $\mathbf{x}$ . Assumption 3 also implies that  $\gamma$  is required to be uniformly bounded away from zero for all  $\mathbf{x}$ ; see [54, Example 3] for examples of functions satisfying Assumption 3. Furthermore, in [54], (6) has been shown to be equivalent to

$$\|\mathbf{H}^\dagger(\mathbf{x})\| \leq \frac{1}{\gamma}. \quad (7)$$

**Assumption 4** (Gradient-Hessian Null-space Property). *For any  $\mathbf{x} \in \mathbb{R}^d$ , let  $\mathbf{U}$  and  $\mathbf{U}_\perp$  denote arbitrary orthogonal bases for  $\text{Range}(\mathbf{H}(\mathbf{x}))$  and its orthogonal complement, respectively. A function is said to satisfy the Gradient-Hessian Null-Space property, if there exists  $0 < \nu \leq 1$ , such that*

$$\|\mathbf{U}_\perp^\top \mathbf{g}(\mathbf{x})\|^2 \leq \left(\frac{1-\nu}{\nu}\right) \|\mathbf{U}^\top \mathbf{g}(\mathbf{x})\|^2, \quad \forall \mathbf{x} \in \mathbb{R}^d. \quad (8)$$

Assumption 4 ensures that the angle between the gradient and the range-space of the Hessian matrix is uniformly bounded away from zero. In other words, as iterations progress, the gradient will not become arbitrarily orthogonal to the range space of Hessian. Explicit examples of functions that satisfy this assumption, including the special case when  $\nu = 1$ , i.e., the gradient lies fully in the range of the full Hessian, are given in [54]. The following lemma, also from [54, Lemma 4], is a direct consequence of Assumption 4.

**Lemma 1** ([54, Lemma 4]). *Under Assumption 4, we have*

$$\|\mathbf{U}^\top \mathbf{g}\|^2 \geq \nu \|\mathbf{g}\|^2, \quad (9a)$$

$$\|\mathbf{U}_\perp^\top \mathbf{g}\|^2 \leq (1-\nu) \|\mathbf{g}\|^2. \quad (9b)$$

## 2 Inexact Hessian and Matrix Perturbation Theory

Typically, at the heart of convergence analysis of various Newton-type methods with inexact Hessian information lies matrix perturbations of the form

$$\tilde{\mathbf{H}} = \mathbf{H} + \mathbf{E}, \quad (10a)$$

for some symmetric matrix  $\mathbf{E}$ . The goal is then to obtain a bound

$$\|\mathbf{E}\| \leq \varepsilon, \quad (10b)$$

such that the algorithm with inexact Hessian has desirable per-iteration costs and yet maintains the iteration complexity of the original exact algorithm. Once such a bound on  $\varepsilon$  is established, a variety

of approaches including deterministic, e.g., finite difference, and stochastic, e.g., sub-sampling, can be used to form  $\tilde{\mathbf{H}}$  in (10). For example, for finite-sum minimization problem (2), [67, Lemma 16] established that if  $|\mathcal{S}| \in \mathcal{O}(\varepsilon^{-2} \log(2d/\delta))$  and samples are drawn uniformly at random, then we have  $\Pr(\|\mathbf{H} - \tilde{\mathbf{H}}\| \leq \varepsilon) \geq 1 - \delta$ . Bounds using non-uniform sampling have also been given, e.g., [67, 69].

In strongly-convex settings, establishing the convergence of the classical Newton’s method and its Newton-CG variant relies on Hessian perturbations that are *approximately spectrum preserving*, e.g.,  $\varepsilon$  in (10) must be such that for the perturbed Hessian, we have

$$(1 - \tilde{\varepsilon}_1)\mathbf{H} \preceq \tilde{\mathbf{H}} \preceq (1 + \tilde{\varepsilon}_1)\mathbf{H}, \quad (11)$$

where  $\tilde{\varepsilon}_1 \in \mathcal{O}(\varepsilon)$ , e.g., [8, 29, 53, 55]. Under (11), the perturbed matrix is not only required to be full-rank, but also it must remain positive definite. In particular, (11) implies that

$$(1 - \tilde{\varepsilon}_2)\mathbf{H}^{-1} \preceq \tilde{\mathbf{H}}^{-1} \preceq (1 + \tilde{\varepsilon}_1)\mathbf{H}^{-1},$$

for some  $\tilde{\varepsilon}_2 \in \mathcal{O}(\varepsilon)$ , which in turn gives

$$\|\mathbf{H}^{-1} - \tilde{\mathbf{H}}^{-1}\| \leq \tilde{\varepsilon}_3, \quad (12)$$

for some  $\tilde{\varepsilon}_3 \in \mathcal{O}(\varepsilon)$  [63, Theorem 2.5], i.e., the inverse of the perturbed Hessian is itself a small perturbation of the inverse of the true Hessian.

In non-convex settings, however, where the true Hessian might be indefinite and/or rank deficient, requiring such conditions is simply infeasible. Indeed, when  $\mathbf{H}$  is indefinite, the inequality (11) ceases to be meaningful, i.e., no value of  $\tilde{\varepsilon} > 0$  can give  $(1 - \tilde{\varepsilon})\mathbf{H} \preceq (1 + \tilde{\varepsilon})\mathbf{H}$ . Further, when  $\mathbf{H}$  has a zero eigenvalue, i.e., it is singular, it is practically impossible to assume that the corresponding eigenvalue of  $\tilde{\mathbf{H}}$  is also zero. In other words, in non-convex settings, no amount of perturbation in (10) will be guaranteed to be spectrum preserving. In such settings, where the Hessian can simply fail to be invertible, one might be tempted to find a similar bound as in (12) but in terms of matrix pseudo-inverse, i.e., to find values of  $\varepsilon$  in (10) such that

$$\|\mathbf{H}^\dagger - \tilde{\mathbf{H}}^\dagger\| \leq \tilde{\varepsilon}_3. \quad (13)$$

However, requiring (13) is also extremely restrictive. In fact, it is known that the necessary and sufficient condition for  $\tilde{\mathbf{H}}^\dagger \rightarrow \mathbf{H}^\dagger$  as  $\tilde{\mathbf{H}} \rightarrow \mathbf{H}$ , i.e., as  $\varepsilon \downarrow 0$ , is that  $\tilde{\mathbf{H}}$  is an *acute perturbation* of  $\mathbf{H}$ , i.e.,  $\text{Rank}(\tilde{\mathbf{H}}) = \text{Rank}(\mathbf{H})$  [63, p. 146]. A cornerstone in the theory of matrix perturbations is establishing conditions on  $\tilde{\mathbf{H}}$  and  $\varepsilon$  in (10) that can give results in the same spirit as (13) for more general perturbations, e.g., [25, 45, 63]. For example, from [63, Theorem 3.8] and (10), we have

$$\|\mathbf{H}^\dagger - \tilde{\mathbf{H}}^\dagger\| \leq \left(\frac{1 + \sqrt{5}}{2}\right) \max\left\{\|\mathbf{H}^\dagger\|^2, \|\tilde{\mathbf{H}}^\dagger\|^2\right\} \varepsilon. \quad (14)$$

Employing (14) to guarantee (13) necessarily relies on assuming  $\|\tilde{\mathbf{H}}^\dagger\| \in o(1/\sqrt{\varepsilon})$ , where “ $o(\cdot)$ ” denotes the “Little-O Notation”, i.e.,  $\|\tilde{\mathbf{H}}^\dagger\|$  must grow at a slower rate than  $1/\sqrt{\varepsilon}$ . However, as demonstrated by the following examples, this assumption is easily violated in many situations.

**Example 1** (Deterministic Perturbations). Suppose  $\|\mathbf{E}\| = \varepsilon$  and that the ratio of the largest over the smallest non-zero singular values of  $\mathbf{E}$  is bounded by some constant, say  $C$ . This, in turn, implies  $\sigma_{r_{\mathbf{E}}}(\mathbf{E}) \geq \varepsilon/C$ , where  $\sigma_{r_{\mathbf{E}}}(\mathbf{E})$  is the smallest non-zero singular value of  $\mathbf{E}$ . Further, suppose that  $r \triangleq \text{Rank}(\mathbf{H}) \leq \text{Rank}(\tilde{\mathbf{H}}) \triangleq \tilde{r}$  (cf. Lemma 2), and  $r_{\mathbf{E}} = \tilde{r} + r$ . By [5, Proposition 9.6.8], we have

$$\sigma_{\tilde{r}}(\tilde{\mathbf{H}}) \geq \sigma_{r_{\mathbf{E}}}(\mathbf{E}) - \sigma_{r+1}(\mathbf{H}) \geq \varepsilon/C,$$

which gives  $\|\tilde{\mathbf{H}}^\dagger\| \in \mathcal{O}(1/\varepsilon)$ .

**Example 2** (Random Perturbations). Suppose  $[\mathbf{E}]_{ij} \sim \mathcal{N}(0, \varepsilon^2)$ , where  $i, j = 1, \dots, d$  and  $\mathcal{N}(0, \varepsilon^2)$  denotes the standard normal distribution with mean zero and standard deviation  $\varepsilon$ . We have  $\sigma_i(\mathbf{H}) = 0$ ,  $d \geq i > r \triangleq \text{Rank}(\mathbf{H})$ . Suppose further that the non-zero singular values of  $\mathbf{H}$  are well separated from zero, e.g.,  $\sigma_i(\mathbf{H}) > 5\varepsilon$ ,  $i = 1, \dots, r$ . Using results similar to [62, p. 411], one can show that the diagonal entries of  $\tilde{\Sigma}_2$  in (22), i.e., the non-zero singular values of  $\tilde{\mathbf{H}}$  corresponding to zero singular values of  $\mathbf{H}$ , will satisfy

$$\mathbb{E} \left[ \sigma_i^2(\tilde{\mathbf{H}}) \right] = (d-r)\varepsilon^2 \quad \text{and} \quad \sigma_i(\tilde{\mathbf{H}}) \leq \sqrt{2} \|\mathbf{E}\|, \quad i = r+1, \dots, d.$$

With probability  $1 - 2\exp(-2d)$ , we have  $\|\mathbf{E}\| \leq 4\sqrt{d}\varepsilon$  [59, Eqn (2.3), p. 1582]. The latter two inequalities alone indicate that assuming  $\sigma_i(\tilde{\mathbf{H}}) \in \Omega(\sqrt{\varepsilon})$ , and hence the stronger condition  $\|\tilde{\mathbf{H}}^\dagger\| \in o(1/\sqrt{\varepsilon})$ , is rather quite unreasonable. Now, on this latter event, for any  $C > 1$ , the reverse Markov inequality gives

$$\Pr \left( \sigma_i(\tilde{\mathbf{H}}) \leq \frac{\varepsilon}{C} \right) \leq \frac{\mathbb{E} \left[ 32d\varepsilon^2 - \sigma_i^2(\tilde{\mathbf{H}}) \right]}{32d\varepsilon^2 - \varepsilon^2/C^2} \leq \frac{32d - (d-r)}{32d - 1/C^2},$$

which implies

$$\Pr \left( \sigma_i(\tilde{\mathbf{H}}) > \frac{\varepsilon}{C} \right) \geq \frac{(d-r) - 1/C^2}{32d - 1/C^2}.$$

In other words, with a positive probability that is independent of  $\varepsilon$ , we have  $\|\tilde{\mathbf{H}}^\dagger\| \in \mathcal{O}(1/\varepsilon)$ .

In light of Examples 1 and 2, a more sensible noise model is the one which allows for  $\|\tilde{\mathbf{H}}^\dagger\|$  to grow at the same rate as  $1/\varepsilon$ .

**Assumption 5** (Perturbation Model). *For the perturbation (10), we have*

$$\left\| \tilde{\mathbf{H}}^\dagger \right\| = \left\| [\mathbf{H} + \mathbf{E}]^\dagger \right\| \leq \frac{C}{\varepsilon}, \quad (15)$$

where  $\varepsilon$  is as in (10) and  $C \geq 1$  is some universal constant.

Under Assumption 5, unless the perturbations are acute, i.e., rank preserving, obtaining (13) is simply hopeless. In this light, instead of considering the distance between  $\mathbf{H}^\dagger$  and  $\tilde{\mathbf{H}}^\dagger$  viewed as linear operators, one can perhaps consider the distance between the subspaces spanned by them respectively. More specifically, instead of (13), one could attempt at finding conditions in (10) such that

$$\left\| \mathbf{U}\mathbf{U}^\top - \tilde{\mathbf{U}}\tilde{\mathbf{U}}^\top \right\| \leq \tilde{\varepsilon}_3, \quad (16)$$

where  $\mathbf{U}$  and  $\tilde{\mathbf{U}}$  are orthonormal bases for  $\text{Range}(\tilde{\mathbf{H}})$  and  $\text{Range}(\mathbf{H})$ , respectively. In other words, at first sight, the quantity of interest could be the distance between the two subspaces, namely  $\text{Range}(\mathbf{H})$  and its perturbation  $\text{Range}(\tilde{\mathbf{H}})$  [32, Section 2.5.3]. More recent and improved results in bounding such distance are given in [50]. For simplicity we include the statement of [50, Theorem 19], but only slightly modified to fit the settings that we consider here.

**Theorem 1** (Modified Davis-Kahan-Wedin Sine Theorem [50, Theorem 19]). *Consider a symmetric matrix  $\mathbf{A} \in \mathbb{R}^{d \times d}$  of rank  $r$ , and let  $\tilde{\mathbf{A}}$  be its symmetric perturbation. For an integer  $1 \leq j \leq r$ , let  $\mathbf{U}_j \triangleq [\mathbf{u}_1, \dots, \mathbf{u}_j] \in \mathbb{R}^{d \times j}$  and  $\tilde{\mathbf{U}}_j \triangleq [\tilde{\mathbf{u}}_1, \dots, \tilde{\mathbf{u}}_j] \in \mathbb{R}^{d \times j}$ , where  $\mathbf{u}_i \in \mathbb{R}^d$  and  $\tilde{\mathbf{u}}_i \in \mathbb{R}^d$  are, respectively,  $i^{\text{th}}$  eigenvectors of matrices  $\mathbf{A}$  and  $\tilde{\mathbf{A}}$ . The principal angle between  $\text{Range}(\mathbf{U}_j)$  and  $\text{Range}(\tilde{\mathbf{U}}_j)$  is given by*

$$\sin \angle \left( \text{Range}(\mathbf{U}), \text{Range}(\tilde{\mathbf{U}}) \right) = \left\| \mathbf{U}_j \mathbf{U}_j^\top - \tilde{\mathbf{U}}_j \tilde{\mathbf{U}}_j^\top \right\| \leq \frac{2 \|\mathbf{A} - \tilde{\mathbf{A}}\|}{\sigma_j(\mathbf{A}) - \sigma_{j+1}(\mathbf{A})}. \quad (17)$$

As a result, if  $\tilde{\mathbf{H}}$  is an acute perturbation of  $\mathbf{H}$ , i.e.,  $\text{Rank}(\tilde{\mathbf{H}}) = \text{Rank}(\mathbf{H}) = r$ , we can appeal to Theorem 1 and obtain a bound as in (16). Indeed, since  $\sigma_{r+1}(\mathbf{H}) = 0$  in this case, we get

$$\left\| \mathbf{U} \mathbf{U}^\top - \tilde{\mathbf{U}} \tilde{\mathbf{U}}^\top \right\| \leq \frac{2 \|\mathbf{H} - \tilde{\mathbf{H}}\|}{\sigma_r(\mathbf{H})} = 2 \|\mathbf{H} - \tilde{\mathbf{H}}\| \|\mathbf{H}^\dagger\| \leq 2 \|\mathbf{H}^\dagger\| \varepsilon.$$

However, from [5, Facts 5.12.17(iv) and 9.9.29], it simply follows that

$$\text{Rank}(\mathbf{H}) \neq \text{Rank}(\tilde{\mathbf{H}}) \implies \left\| \tilde{\mathbf{U}} \tilde{\mathbf{U}}^\top - \mathbf{U} \mathbf{U}^\top \right\| = 1.$$

Again as before, requiring (16) in non-convex settings is indeed far too stringent.

What comes to the rescue is the observation that instead of obtaining a bound as in (16), which implies a bounded distance between  $\mathbf{U} \mathbf{U}^\top$  and  $\tilde{\mathbf{U}} \tilde{\mathbf{U}}^\top$  along *every* direction, for Newton-MR, we only need such distance to be bounded along a *specific* direction, i.e., that of the gradient  $\mathbf{g}$ . Indeed, instead of (16), which implies

$$\left\| \left( \mathbf{H} \mathbf{H}^\dagger - \tilde{\mathbf{H}} \tilde{\mathbf{H}}^\dagger \right) \mathbf{v} \right\| \leq \tilde{\varepsilon} \|\mathbf{v}\|, \quad \forall \mathbf{v} \in \mathbb{R}^d,$$

by only considering  $\mathbf{v} = \mathbf{g}$  in the above, we seek to bound only the projection of the gradient on the range space of the Hessian matrices as

$$\left\| \left( \mathbf{H} \mathbf{H}^\dagger - \tilde{\mathbf{H}} \tilde{\mathbf{H}}^\dagger \right) \mathbf{g} \right\| \leq \tilde{\varepsilon} \|\mathbf{g}\|. \quad (18)$$

We now set out to obtain conditions that can guarantee (18). Our result relies on the following lemma (Lemma 2), which establishes a relationship between  $\varepsilon$  in (10) and  $\text{Rank}(\tilde{\mathbf{H}})$ . Although assuming rank-preserving perturbation, i.e.,  $\text{Rank}(\mathbf{H}_k) = \text{Rank}(\tilde{\mathbf{H}}_k)$ , is too stringent to be of any practical use, under certain conditions, we can ensure that the perturbed matrix has a rank at least as large as the original matrix, i.e., perturbation is such that the rank is, at least, not reduced.

**Lemma 2** (Rank of Perturbed Hessian). *Under Assumption 3, if  $\varepsilon < \gamma$  in (10), then  $\text{Rank}(\tilde{\mathbf{H}}) \geq \text{Rank}(\mathbf{H})$ .*

*Proof.* First note that from (10), it follows that  $\lambda_{\min}(\tilde{\mathbf{H}} - \mathbf{H}) \geq -\varepsilon$ , and  $\lambda_{\max}(\tilde{\mathbf{H}} - \mathbf{H}) \leq \varepsilon$ . Let  $r = \text{Rank}(\mathbf{H})$  and  $\tilde{r} = \text{Rank}(\tilde{\mathbf{H}})$ . By [5, Theorem 8.4.11], for any  $1 \leq j \leq r$ , we have

$$\lambda_j(\mathbf{H}) + \lambda_{\min}(\tilde{\mathbf{H}} - \mathbf{H}) \leq \lambda_j(\tilde{\mathbf{H}}) \leq \lambda_j(\mathbf{H}) + \lambda_{\max}(\tilde{\mathbf{H}} - \mathbf{H}),$$

which implies

$$\lambda_j(\mathbf{H}) - \varepsilon \leq \lambda_j(\tilde{\mathbf{H}}) \leq \lambda_j(\mathbf{H}) + \varepsilon. \quad (19)$$

Now Assumption 3 implies that  $|\lambda_j(\mathbf{H})| \geq \gamma$ ,  $1 \leq j \leq r$ . Hence, we get

$$\begin{aligned} \lambda_j(\tilde{\mathbf{H}}) &\leq \lambda_j(\mathbf{H}) + \varepsilon \leq -\gamma + \varepsilon < 0, & \text{if } \lambda_j(\mathbf{H}) < 0, \\ \lambda_j(\tilde{\mathbf{H}}) &\geq \lambda_j(\mathbf{H}) - \varepsilon \geq \gamma - \varepsilon > 0, & \text{if } \lambda_j(\mathbf{H}) > 0. \end{aligned}$$

Thus, it follows that  $\lambda_j(\tilde{\mathbf{H}}) \neq 0, \forall j = 1, \dots, r$ , which implies that  $\text{Rank}(\tilde{\mathbf{H}}) \geq \text{Rank}(\mathbf{H})$ .  $\square$

Lemma 2 states that if  $\varepsilon < \gamma$ , the perturbed Hessian is never of lower rank than the original Hessian. In other words, if  $\text{Rank}(\tilde{\mathbf{H}}) < \text{Rank}(\mathbf{H})$ , then we must necessarily have that  $\varepsilon \geq \gamma$ . Also, from the proof of Lemma 2 and using the fact that  $\tilde{\mathbf{H}}$  is symmetric, we have

$$\sigma_i(\tilde{\mathbf{H}}) \geq \gamma - \varepsilon, \quad i = 1, \dots, r, \quad (20)$$

where  $\gamma$  is as in Assumption 3. Furthermore, if  $\varepsilon < \gamma$ , we have  $r < \tilde{r}$ , which by (15) and (19) yields

$$\frac{\varepsilon}{C} \leq \sigma_i(\tilde{\mathbf{H}}) \leq \varepsilon, \quad i = r + 1, \dots, \tilde{r}. \quad (21)$$

For the remainder of this paper, with  $r \leq \tilde{r}$ , we let the singular value decomposition of  $\mathbf{H}$  and  $\tilde{\mathbf{H}}$  be

$$\mathbf{H} = [\mathbf{U} \quad \mathbf{U}_\perp] \begin{bmatrix} \Sigma & 0 \\ 0 & 0 \end{bmatrix} \mathbf{V}^\top, \quad \text{and} \quad \tilde{\mathbf{H}} = \underbrace{[\tilde{\mathbf{U}}_1 \quad \tilde{\mathbf{U}}_2 \quad \tilde{\mathbf{U}}_\perp]}_{\tilde{\mathbf{U}}} \begin{bmatrix} \tilde{\Sigma}_1 & 0 & 0 \\ 0 & \tilde{\Sigma}_2 & 0 \\ 0 & 0 & 0 \end{bmatrix} \tilde{\mathbf{V}}^\top, \quad (22)$$

where

$$\begin{aligned} \mathbf{U} &\in \mathbb{R}^{d \times r}, \Sigma \in \mathbb{R}^{r \times r}, \mathbf{V} \in \mathbb{R}^{d \times d}, \\ \tilde{\mathbf{U}}_1 &\in \mathbb{R}^{d \times r}, \tilde{\mathbf{U}}_2 \in \mathbb{R}^{d \times (\tilde{r} - r)}, \tilde{\Sigma}_1 \in \mathbb{R}^{r \times r}, \tilde{\Sigma}_2 \in \mathbb{R}^{(\tilde{r} - r) \times (\tilde{r} - r)}, \tilde{\mathbf{V}} \in \mathbb{R}^{d \times d}. \end{aligned}$$

Note that  $\tilde{\mathbf{U}} \in \mathbb{R}^{d \times \tilde{r}}$  is divided into  $\tilde{\mathbf{U}}_1 \in \mathbb{R}^{d \times r}$  and  $\tilde{\mathbf{U}}_2 \in \mathbb{R}^{d \times (\tilde{r} - r)}$ . Furthermore,  $\mathbf{U}$  and  $\tilde{\mathbf{U}}_1$  have the same rank. Now, using Lemma 2, we can establish (18).

**Theorem 2.** *Under Assumptions 3 and 4, and with  $\varepsilon < \gamma$  in (10), we have (18) with*

$$\tilde{\varepsilon} \triangleq \frac{4\varepsilon}{\gamma} + \sqrt{1 - \nu}.$$

*Furthermore, in special case of acute perturbation, i.e.,  $\text{Rank}(\mathbf{H}) = \text{Rank}(\tilde{\mathbf{H}})$ , we have*

$$\tilde{\varepsilon} \triangleq \frac{2\varepsilon}{\gamma}.$$

*Here,  $\gamma$  and  $\nu$  are as in Assumptions 3 and 4, respectively.*

*Proof.* By assumption on  $\varepsilon$ , Lemma 2 gives  $r \triangleq \text{Rank}(\mathbf{H}) \leq \text{Rank}(\tilde{\mathbf{H}}) \triangleq \tilde{r}$ . By (7), (9b), and (17), we will have

$$\begin{aligned} \left\| \mathbf{H}\mathbf{H}^\dagger \mathbf{g} - \tilde{\mathbf{H}}\tilde{\mathbf{H}}^\dagger \mathbf{g} \right\| &= \left\| \mathbf{U}\mathbf{U}^\top \mathbf{g} - \tilde{\mathbf{U}}\tilde{\mathbf{U}}^\top \mathbf{g} \right\| \leq \left\| \mathbf{U}\mathbf{U}^\top \mathbf{g} - \tilde{\mathbf{U}}_1\tilde{\mathbf{U}}_1^\top \mathbf{g} \right\| + \left\| \tilde{\mathbf{U}}_2\tilde{\mathbf{U}}_2^\top \mathbf{g} \right\| \\ &\leq \left\| \mathbf{U}\mathbf{U}^\top \mathbf{g} - \tilde{\mathbf{U}}_1\tilde{\mathbf{U}}_1^\top \mathbf{g} \right\| + \left\| \tilde{\mathbf{U}}_2\tilde{\mathbf{U}}_2^\top \mathbf{g} + \tilde{\mathbf{U}}_\perp\tilde{\mathbf{U}}_\perp^\top \mathbf{g} \right\| \\ &= \left\| \mathbf{U}\mathbf{U}^\top \mathbf{g} - \tilde{\mathbf{U}}_1\tilde{\mathbf{U}}_1^\top \mathbf{g} \right\| + \left\| \tilde{\mathbf{U}}_2\tilde{\mathbf{U}}_2^\top \mathbf{g} + \tilde{\mathbf{U}}_\perp\tilde{\mathbf{U}}_\perp^\top \mathbf{g} - \mathbf{U}_\perp\mathbf{U}_\perp^\top \mathbf{g} + \mathbf{U}_\perp\mathbf{U}_\perp^\top \mathbf{g} \right\| \\ &= \left\| \mathbf{U}\mathbf{U}^\top \mathbf{g} - \tilde{\mathbf{U}}_1\tilde{\mathbf{U}}_1^\top \mathbf{g} \right\| + \left\| (\mathbf{I} - \mathbf{U}_\perp\mathbf{U}_\perp^\top) \mathbf{g} - (\mathbf{I} - \tilde{\mathbf{U}}_2\tilde{\mathbf{U}}_2^\top - \tilde{\mathbf{U}}_\perp\tilde{\mathbf{U}}_\perp^\top) \mathbf{g} + \mathbf{U}_\perp\mathbf{U}_\perp^\top \mathbf{g} \right\| \\ &\leq \left\| \mathbf{U}\mathbf{U}^\top \mathbf{g} - \tilde{\mathbf{U}}_1\tilde{\mathbf{U}}_1^\top \mathbf{g} \right\| + \left\| (\mathbf{I} - \mathbf{U}_\perp\mathbf{U}_\perp^\top) \mathbf{g} - (\mathbf{I} - \tilde{\mathbf{U}}_2\tilde{\mathbf{U}}_2^\top - \tilde{\mathbf{U}}_\perp\tilde{\mathbf{U}}_\perp^\top) \mathbf{g} \right\| + \left\| \mathbf{U}_\perp\mathbf{U}_\perp^\top \mathbf{g} \right\| \\ &\leq 2 \left\| \mathbf{U}\mathbf{U}^\top \mathbf{g} - \tilde{\mathbf{U}}_1\tilde{\mathbf{U}}_1^\top \mathbf{g} \right\| + \left\| \mathbf{U}_\perp\mathbf{U}_\perp^\top \mathbf{g} \right\| \\ &\leq 4 \left\| \mathbf{H} - \tilde{\mathbf{H}} \right\| \left\| \mathbf{H}^\dagger \right\| \left\| \mathbf{g} \right\| + \sqrt{1 - \nu} \left\| \mathbf{g} \right\| \\ &\leq \left( \frac{4\varepsilon}{\gamma} + \sqrt{1 - \nu} \right) \left\| \mathbf{g} \right\|, \end{aligned}$$



where in the second inequality, we used the Pythagorean theorem as

$$\left\| \tilde{\mathbf{U}}_2 \tilde{\mathbf{U}}_2^\top \mathbf{g} + \tilde{\mathbf{U}}_\perp \tilde{\mathbf{U}}_\perp^\top \mathbf{g} \right\|^2 = \left\| \tilde{\mathbf{U}}_2 \tilde{\mathbf{U}}_2^\top \mathbf{g} \right\|^2 + \left\| \tilde{\mathbf{U}}_\perp \tilde{\mathbf{U}}_\perp^\top \mathbf{g} \right\|^2 \geq \left\| \tilde{\mathbf{U}}_2 \tilde{\mathbf{U}}_2^\top \mathbf{g} \right\|^2,$$

and for the last equality we use the fact that  $\mathbf{U}\mathbf{U}^\top + \mathbf{U}_\perp \mathbf{U}_\perp^\top = \mathbf{I}$ , and  $\tilde{\mathbf{U}}_1 \tilde{\mathbf{U}}_1^\top + \tilde{\mathbf{U}}_2 \tilde{\mathbf{U}}_2^\top + \tilde{\mathbf{U}}_\perp \tilde{\mathbf{U}}_\perp^\top = \mathbf{I}$ . The special case of acute perturbation follows simply from the above without the term involving  $\left\| \tilde{\mathbf{U}}_2 \tilde{\mathbf{U}}_2^\top \mathbf{g} \right\|$ .  $\square$

Theorem 2 also allows us to obtain results similar in spirit to Lemma 1.

**Lemma 3.** *Under assumptions of Theorem 2, we have*

$$\left\| \tilde{\mathbf{U}}^\top \mathbf{g} \right\|^2 \geq \tilde{\nu} \|\mathbf{g}\|^2, \quad (23a)$$

$$\left\| \tilde{\mathbf{U}}_\perp^\top \mathbf{g} \right\|^2 \leq (1 - \tilde{\nu}) \|\mathbf{g}\|^2, \quad (23b)$$

where

$$\tilde{\nu} \triangleq 2\nu - 1 - \frac{4\varepsilon}{\gamma},$$

and  $0.5 < \nu \leq 1$ ,  $\varepsilon < \gamma(2\nu - 1)/4$ . Furthermore, in the special case of acute perturbation, i.e.,  $\text{Rank}(\mathbf{H}) = \text{Rank}(\tilde{\mathbf{H}})$ , we have (23) with

$$\tilde{\nu} \triangleq \nu - \frac{2\varepsilon}{\gamma},$$

where  $0 < \nu \leq 1$ ,  $\varepsilon < \gamma\nu/2$ . Here,  $\gamma$  is as in (6), and  $\tilde{\mathbf{U}}, \tilde{\mathbf{U}}_\perp$  are as in (22).

*Proof.* We have.

$$\left\| \tilde{\mathbf{U}}^\top \mathbf{g} \right\|^2 = \mathbf{g}^\top \tilde{\mathbf{U}} \tilde{\mathbf{U}}^\top \mathbf{g} = \mathbf{g}^\top \mathbf{U} \mathbf{U}^\top \mathbf{g} - \mathbf{g}^\top (\mathbf{U} \mathbf{U}^\top - \tilde{\mathbf{U}} \tilde{\mathbf{U}}^\top) \mathbf{g}.$$

Similarly to the proof of Theorem 2 and using Lemma 1, we have

$$\begin{aligned} \left| \mathbf{g}^\top \mathbf{U} \mathbf{U}^\top \mathbf{g} - \mathbf{g}^\top \tilde{\mathbf{U}} \tilde{\mathbf{U}}^\top \mathbf{g} \right| &\leq \left| \mathbf{g}^\top \mathbf{U} \mathbf{U}^\top \mathbf{g} - \mathbf{g}^\top \tilde{\mathbf{U}}_1 \tilde{\mathbf{U}}_1^\top \mathbf{g} \right| + \left| \mathbf{g}^\top \tilde{\mathbf{U}}_2 \tilde{\mathbf{U}}_2^\top \mathbf{g} \right| \leq \frac{2\varepsilon}{\gamma} + \mathbf{g}^\top \tilde{\mathbf{U}}_2 \tilde{\mathbf{U}}_2^\top \mathbf{g} \\ &\leq \frac{2\varepsilon}{\gamma} + \left| \mathbf{g}^\top \mathbf{U} \mathbf{U}^\top \mathbf{g} - \mathbf{g}^\top \tilde{\mathbf{U}}_1 \tilde{\mathbf{U}}_1^\top \mathbf{g} \right| + \mathbf{g}^\top \mathbf{U}_\perp \mathbf{U}_\perp^\top \mathbf{g} \leq \left( \frac{4\varepsilon}{\gamma} + 1 - \nu \right) \|\mathbf{g}\|^2. \end{aligned}$$

Now, it follows that

$$\left\| \tilde{\mathbf{U}}^\top \mathbf{g} \right\|^2 \geq \mathbf{g}^\top \mathbf{U} \mathbf{U}^\top \mathbf{g} - \left( \frac{4\varepsilon}{\gamma} + 1 - \nu \right) \|\mathbf{g}\|^2 \geq \left( 2\nu - 1 - \frac{4\varepsilon}{\gamma} \right) \|\mathbf{g}\|^2,$$

which gives (23a). Now noting that  $\|\mathbf{g}\|^2 = \left\| \tilde{\mathbf{U}}^\top \mathbf{g} \right\|^2 + \left\| \tilde{\mathbf{U}}_\perp^\top \mathbf{g} \right\|^2$ , we get (23b). Finally, for the case of acute perturbations, since  $\tilde{\mathbf{U}} \tilde{\mathbf{U}}^\top = \tilde{\mathbf{U}}_1 \tilde{\mathbf{U}}_1^\top$  (recall that in this case  $\tilde{\Sigma}_2 = \mathbf{0}$ ), it follows that

$$\left| \mathbf{g}^\top \mathbf{U} \mathbf{U}^\top \mathbf{g} - \mathbf{g}^\top \tilde{\mathbf{U}} \tilde{\mathbf{U}}^\top \mathbf{g} \right| = \left| \mathbf{g}^\top \mathbf{U} \mathbf{U}^\top \mathbf{g} - \mathbf{g}^\top \tilde{\mathbf{U}}_1 \tilde{\mathbf{U}}_1^\top \mathbf{g} \right| \leq \frac{2\varepsilon}{\gamma} \|\mathbf{g}\|^2.$$

which gives the desired result.  $\square$

As it is evident from Theorem 2, situations where either  $\nu = 1$  or the perturbation is acute, exhibit a certain inherent stability. More specifically, define the operator  $\boldsymbol{\pi} : \mathbb{R}^{d \times d} \rightarrow \mathbb{R}^d$  as  $\boldsymbol{\pi}(\mathbf{E}) \triangleq (\mathbf{H} + \mathbf{E})(\mathbf{H} + \mathbf{E})^\dagger \mathbf{g} = \tilde{\mathbf{H}} \tilde{\mathbf{H}}^\dagger \mathbf{g}$ , i.e., the projection of the gradient onto the range space of  $\tilde{\mathbf{H}} = \mathbf{H} + \mathbf{E}$ . When  $\nu = 1$  or the perturbation is acute, such a mapping is continuous at  $\mathbf{E} = \mathbf{0}$ , i.e.,  $\lim_{\|\mathbf{E}\| \rightarrow 0} \boldsymbol{\pi}(\mathbf{E}) = \boldsymbol{\pi}(\mathbf{0}) = \mathbf{H} \mathbf{H}^\dagger \mathbf{g}$ . This observation gives rise to the following definition.

**Definition 1** (Inherent Stability). *A perturbation remains inherently stable if one of the following conditions hold:*

- $\tilde{\mathbf{H}}$  is an acute perturbation of  $\mathbf{H}$ , i.e.,  $\text{Rank}(\tilde{\mathbf{H}}) = \text{Rank}(\mathbf{H})$ , or
- $\nu = 1$  with  $\nu$  as in Assumption 4, i.e.,  $\mathbf{g} \in \text{Range}(\mathbf{H})$ .

In light of Definition 1 and Lemma 3, we end this section by specifically stating the perturbation regimes where we develop our convergence theory of Section 3.

**Condition 1.** *We consider two perturbation regimes:*

- For general perturbations, we consider (10) with  $\varepsilon < \gamma(2\nu - 1)/4$  for  $0.5 < \nu \leq 1$ .
  - For inherently stable perturbations, we consider (10) with  $\varepsilon < \gamma\nu/2$  for  $0 < \nu \leq 1$ .
- Here,  $\gamma$  and  $\nu$  are, respectively, as in Assumptions 3 and 4.

### 3 Newton-MR with Hessian Approximations

In this section, we provide convergence analysis of Newton-MR with inexact Hessian. To do so, we first briefly review Newton-MR in Section 3.1 and, in its light, introduce the variant in which the Hessian is approximated (Algorithm 1). This is then followed by its convergence analysis in Section 3.2. For the special case of strongly-convex problems, the convergence results of Section 3.2 bear a strong resemblance to those of the classical Newton’s method (and Newton-CG variant) with inexact Hessian, e.g., [8, 55]. These comparisons are made in more details in Section 3.3.

#### 3.1 Newton-MR Algorithm: Review

We now briefly review Newton-MR as it was introduced in [54]. In non-convex settings, the Hessian matrix could be indefinite and possibly rank-deficient. In this light, at the  $k^{\text{th}}$  iteration, Newton-MR in its pure form involves the exact update direction of the form

$$\mathbf{p}_k = -[\mathbf{H}_k]^\dagger \mathbf{g}_k. \quad (24)$$

The exact update direction (24) can be equivalently written as the least norm solution to the least squares problem  $\|\mathbf{g}_k + \mathbf{H}_k \mathbf{p}\|$ , i.e.,

$$\min_{\mathbf{p} \in \mathbb{R}^d} \|\mathbf{p}\| \quad \text{subject to} \quad \mathbf{p} \in \text{Arg min}_{\hat{\mathbf{p}} \in \mathbb{R}^d} \|\mathbf{H}_k \hat{\mathbf{p}} + \mathbf{g}_k\|. \quad (25)$$

In practice, computing the Moore-Penrose generalized inverse can be computationally prohibitive, in which case the inexact variant of Newton-MR makes use of approximate update direction as

$$\text{Find } \mathbf{p}_k \in \text{Range}(\mathbf{H}_k), \quad \text{subject to} \quad \langle \mathbf{p}_k, \mathbf{H}_k \mathbf{g}_k \rangle \leq -(1 - \theta) \|\mathbf{g}_k\|^2, \quad (26)$$

where  $\theta < 1$  is the inexactness tolerance. It is easy to see that (26) is implied by (25). When  $\mathbf{g}_k \in \text{Range}(\mathbf{H}_k)$ , i.e., the linear system  $\mathbf{H}_k \mathbf{p} = -\mathbf{g}_k$  is consistent, MINRES [51] can be used to obtain (approximate) pseudo-inverse solution. However, due to its many desirable properties, MINRES-QLP [21] has been advocated in [54] for more general cases as the preferred solver for (25) or (26). When the Hessian is perturbed, even if initially  $\mathbf{g}_k \in \text{Range}(\mathbf{H}_k)$ , it is generally most likely that  $\mathbf{g}_k \notin \text{Range}(\tilde{\mathbf{H}}_k)$ , and hence MINRES-QLP remains the method of choice for our setting here.

After computing the update direction, the next iterate is obtained by moving along  $\mathbf{p}_k$  by some appropriate step length, i.e.,  $\mathbf{x}_{k+1} = \mathbf{x}_k + \alpha_k \mathbf{p}_k$ . Note that from both (25) and (26) it follows that  $\langle \mathbf{p}_k, \mathbf{H}_k \mathbf{g}_k \rangle \leq 0$ , i.e.,  $\mathbf{p}_k$  is a descent direction for the norm of the gradient,  $\|\mathbf{g}\|^2$ . As a result, the step-size,  $\alpha_k$ , can be chosen by applying Armijo-type line-search [49] such that for some  $0 \leq \alpha_k \leq 1$ , we have

$$\|\mathbf{g}_{k+1}\|^2 \leq \|\mathbf{g}_k\|^2 + 2\rho\alpha_k \langle \mathbf{p}_k, \mathbf{H}_k \mathbf{g}_k \rangle, \quad (27)$$

where  $0 < \rho < 1$  is a given line-search parameter. Typically, back-tracking strategy [49] is employed to approximately find such a step-size.

Modification of Newton-MR to include the perturbed matrix  $\tilde{\mathbf{H}}$  as in (10b) is rather straightforward. We simply replace  $\mathbf{H}_k$  with  $\tilde{\mathbf{H}}_k$  in all of (25) to (27). The modified variant is depicted in Algorithm 1. Note that, in this context, whenever we refer to (25), (26) and (27), it is implied that  $\tilde{\mathbf{H}}$  is used instead of  $\mathbf{H}$ .

---

**Algorithm 1** Newton-MR With Inexact Hessian Information

---

- 1: **Input:**  $\mathbf{x}_0$ ,  $0 < \tau < 1$ ,  $0 < \rho < 1$
  - 2: **for**  $k = 0, 1, 2, \dots$  until  $\|\mathbf{g}_k\| \leq \tau$  **do**
  - 3:   Solve (25) (or (26) with MINRES-QLP) with  $\tilde{\mathbf{H}}_k$  in place of  $\mathbf{H}_k$
  - 4:   Find  $\alpha_k$  such that (27) holds with  $\tilde{\mathbf{H}}_k$  in place of  $\mathbf{H}_k$
  - 5:   Update  $\mathbf{x}_{k+1} = \mathbf{x}_k + \alpha_k \mathbf{p}_k$
  - 6: **end for**
  - 7: **Output:**  $\mathbf{x}$  for which  $\|\mathbf{g}_k\| \leq \tau$
- 

## 3.2 Convergence Analysis

In this section, we give the convergence analysis of Algorithm 1. For this, in Section 3.2.1 we first consider the exact update (25), and subsequently in Section 3.2.2, consider the inexact variant where the update direction is computed approximately using (26).

### 3.2.1 Exact Updates

A major ingredient in establishing the convergence of Algorithm 1 using (25) is to obtain an upper-bound on the norm of the exact updates,  $\mathbf{p} = -\tilde{\mathbf{H}}^\dagger \mathbf{g}$ . This indeed is crucial in light of (15), which implies that  $\tilde{\mathbf{H}}^\dagger$  can grow unbounded as  $\varepsilon \downarrow 0$ . However, as in Theorem 2, we can obtain a bound, which fits squarely into the notion of inherently stable perturbations from Definition 1.

**Lemma 4** (Stability of Pseudo-inverse of Perturbed Hessian). *Under Assumption 5 as well as Assumptions of Theorem 2, we have*

$$\|\tilde{\mathbf{H}}^\dagger \mathbf{g}\| \leq \frac{1}{\tilde{\gamma}} \|\mathbf{g}\|,$$

where

$$\tilde{\gamma} \triangleq \left( \frac{1}{\gamma - \varepsilon} + C \left( \frac{2}{\gamma} + \frac{\sqrt{1 - \nu}}{\varepsilon} \right) \right)^{-1}.$$

Furthermore, in special case of acute perturbation, i.e.,  $\text{Rank}(\mathbf{H}) = \text{Rank}(\tilde{\mathbf{H}})$ , we have

$$\tilde{\gamma} \triangleq \gamma - \varepsilon.$$

Here,  $\gamma, \nu, \varepsilon$  and  $C$  are, respectively, as in (6), (8), (10) and (15).

*Proof.* Consider the SVD of  $\tilde{\mathbf{H}}^\dagger$  as in (22). Note that (20) implies that  $\|\tilde{\Sigma}_1^{-1}\| \leq 1/(\gamma - \varepsilon)$ . Further,

from (21), it follows that  $\|\tilde{\Sigma}_2^{-1}\| \leq C/\varepsilon$ . Now, it follows that

$$\begin{aligned} \|\tilde{\mathbf{H}}^\dagger \mathbf{g}\|^2 &= \left\| \tilde{\mathbf{V}} \begin{bmatrix} \tilde{\Sigma}_1^{-1} & 0 & 0 \\ 0 & \tilde{\Sigma}_2^{-1} & 0 \\ 0 & 0 & 0 \end{bmatrix} \begin{bmatrix} \tilde{\mathbf{U}}_1^\top \\ \tilde{\mathbf{U}}_2^\top \\ \tilde{\mathbf{U}}_\perp^\top \end{bmatrix} \mathbf{g} \right\|^2 \\ &= \left\| \tilde{\Sigma}_1^{-1} \tilde{\mathbf{U}}_1^\top \mathbf{g} \right\|^2 + \left\| \tilde{\Sigma}_2^{-1} \tilde{\mathbf{U}}_2^\top \mathbf{g} \right\|^2 \\ &\leq \frac{1}{(\gamma - \varepsilon)^2} \|\mathbf{g}\|^2 + C^2 \left( \frac{2}{\gamma} + \frac{\sqrt{1-\nu}}{\varepsilon} \right)^2 \|\mathbf{g}\|^2, \end{aligned}$$

where the last inequality is obtained using the bound on  $\|\tilde{\mathbf{U}}_2^\top \mathbf{g}\| = \|\tilde{\mathbf{U}}_2 \tilde{\mathbf{U}}_2^\top \mathbf{g}\|$  as in the proof of Theorem 2. The result follows from the inequality  $\sqrt{a^2 + b^2} \leq a + b$ ,  $\forall a, b \geq 0$ .  $\square$

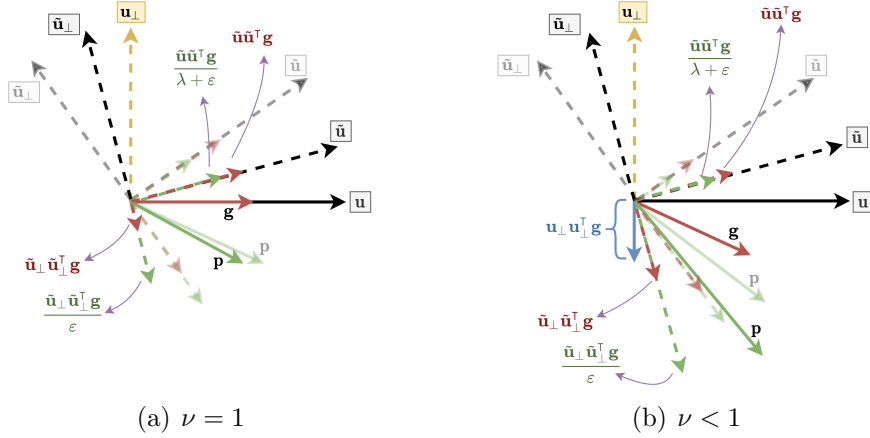


Figure 1: Illustration of Lemma 4 for non-acute perturbations when  $\text{Rank}(\mathbf{H}) = 1$  and  $d = 2$ . Here  $\text{Span}\{\mathbf{u}\} = \text{Range}(\mathbf{H})$ ,  $\text{Span}\{\mathbf{u}_\perp\} = \text{Null}(\mathbf{H})$ ,  $\lambda$  is the non-zero eigenvalue of  $\mathbf{H}$ ,  $\{\tilde{\mathbf{u}}, \tilde{\mathbf{u}}_\perp\}$  are the eigenvectors of  $\tilde{\mathbf{H}}$  and  $\text{Rank}(\tilde{\mathbf{H}}) = 2$ . Also,  $\mathbf{p} = \tilde{\mathbf{H}}^\dagger \mathbf{g} = \tilde{\mathbf{u}}\tilde{\mathbf{u}}^\top \mathbf{g}/\tilde{\lambda} + \tilde{\mathbf{u}}_\perp \tilde{\mathbf{u}}_\perp^\top \mathbf{g}/\varepsilon$ , where  $\tilde{\lambda} \in \lambda \pm \mathcal{O}(\varepsilon)$  (here, we assume  $\lambda \geq 1$  and, for simplicity,  $\tilde{\lambda} = \lambda + \varepsilon$ ). The transparent arrows depict the case for the larger  $\varepsilon$  while the opaque ones correspond to the smaller  $\varepsilon$ . (a) When  $\nu = 1$ ,  $\mathbf{g}$  lies entirely along  $\mathbf{u}$ . Hence, its projections on  $\tilde{\mathbf{u}}_\perp$  will shrink to zero as  $\varepsilon \downarrow 0$ , and  $\lim_{\varepsilon \downarrow 0} \|\tilde{\mathbf{u}}_\perp \tilde{\mathbf{u}}_\perp^\top \mathbf{g}\|/\varepsilon \in \mathcal{O}(1)$ . (b) When  $\nu < 1$ ,  $\mathbf{g}$  has non-zero components along  $\mathbf{u}_\perp$ . Hence, its projections on  $\tilde{\mathbf{u}}_\perp$  will be bounded away from zero, i.e.,  $\lim_{\varepsilon \downarrow 0} \tilde{\mathbf{u}}_\perp \tilde{\mathbf{u}}_\perp^\top \mathbf{g} = \mathbf{u}_\perp \mathbf{u}_\perp^\top \mathbf{g}$ , and  $\|\tilde{\mathbf{u}}_\perp \tilde{\mathbf{u}}_\perp^\top \mathbf{g}\|/\varepsilon \rightarrow \infty$  as  $\varepsilon \downarrow 0$ . As a result, when  $\varepsilon \downarrow 0$ , this component of  $\mathbf{p}$  grows unboundedly.

**Remark 1.** As indicated in Section 2, obtaining a bound similar to (7) for  $\tilde{\mathbf{H}}$  is entirely dependent on having  $\text{Rank}(\mathbf{H}) = \text{Rank}(\tilde{\mathbf{H}})$ , which is too stringent to require. Lemma 4 indicates that, when  $\text{Rank}(\mathbf{H}) \neq \text{Rank}(\tilde{\mathbf{H}})$ , despite the fact that  $\|\tilde{\mathbf{H}}^\dagger\|$  can grow unbounded as  $\varepsilon \downarrow 0$ , if  $\nu = 1$ , we are guaranteed that the action of  $\tilde{\mathbf{H}}^\dagger$  on  $\mathbf{g}$ , i.e., the exact Newton-MR direction, indeed remains bounded. If  $\nu < 1$  and  $\text{Rank}(\mathbf{H}) \neq \text{Rank}(\tilde{\mathbf{H}})$ , then  $\|\tilde{\mathbf{H}}^\dagger \mathbf{g}\|$  can become increasingly larger with smaller perturbations, resulting in an algorithm that might no longer converge; see the numerical examples of Section 4.1. An intuitive illustration of this phenomenon is also depicted in Figure 1.

For our convergence proofs, we frequently make use of the following result.

**Lemma 5** ([54, Lemma 10]). *Consider any  $\mathbf{x}, \mathbf{z} \in \mathbb{R}^d$ ,  $0 \leq L < \infty$  and  $h : \mathbb{R}^d \rightarrow \mathbb{R}$ . If it holds that  $\|\nabla h(\mathbf{y}) - \nabla h(\mathbf{x})\| \leq L \|\mathbf{y} - \mathbf{x}\|$ ,  $\forall \mathbf{y} \in [\mathbf{x}, \mathbf{z}]$ , then, we have  $h(\mathbf{y}) \leq h(\mathbf{x}) + \langle \nabla h(\mathbf{x}), \mathbf{y} - \mathbf{x} \rangle +$*

$$L \|\mathbf{y} - \mathbf{x}\|^2 / 2, \forall \mathbf{y} \in [\mathbf{x}, \mathbf{z}].$$

If we take  $h(\mathbf{x}) = \|\mathbf{g}(\mathbf{x})\|^2 / 2$ , the constant  $L$  in Lemma 5 is  $L(\mathbf{x}_0)$  in Assumption 2.

We now establish a general structural result, which allows for obtaining sufficient conditions for convergence of Algorithm 1.

**Theorem 3** (Algorithm 1 With Exact Updates). *Under Assumptions 1 to 5 and Condition 1, for the iterates of Algorithm 1 with exact updates (25), we have*

$$\|\mathbf{g}_{k+1}\|^2 \leq (1 - \eta) \|\mathbf{g}_k\|^2,$$

where

$$\eta \triangleq \max \left\{ 0, \frac{4\rho\tilde{\nu}\tilde{\gamma}^2}{L(\mathbf{x}_0)} \left( (1 - \rho)\tilde{\nu} - \frac{\varepsilon}{\tilde{\gamma}} \right) \right\} \in [0, 1],$$

and  $\rho, L(\mathbf{x}_0), \tilde{\nu}$  and  $\tilde{\gamma}$  are, respectively, as in (27), Assumption 2, and Lemmas 3 and 4.

*Proof.* From Lemma 5 with  $\mathbf{x} = \mathbf{x}_k$ ,  $\mathbf{z} = \mathbf{x}_k + \mathbf{p}_k$ ,  $\mathbf{y} = \mathbf{x}_k + \alpha\mathbf{p}_k$ , and  $h(\mathbf{x}) = \|\mathbf{g}(\mathbf{x})\|^2 / 2$ , we have

$$\|\mathbf{g}_{k+1}\|^2 \leq \|\mathbf{g}_k\|^2 + 2\alpha \langle \mathbf{p}_k, \mathbf{H}_k \mathbf{g}_k \rangle + \alpha^2 L(\mathbf{x}_0) \|\mathbf{p}_k\|^2 \quad (28)$$

Now to obtain a sufficient condition on  $\alpha$  to satisfy (27), we consider the inequality

$$2\alpha \langle \mathbf{p}_k, \mathbf{H}_k \mathbf{g}_k \rangle + \alpha^2 L(\mathbf{x}_0) \|\mathbf{p}_k\|^2 \leq 2\rho\alpha \langle \mathbf{p}_k, \tilde{\mathbf{H}}_k \mathbf{g}_k \rangle,$$

we used (28) as upper bound on  $\|\mathbf{g}_{k+1}\|^2$ . Rearranging gives

$$\alpha \leq \frac{2 \left( \rho \langle \mathbf{g}_k, \tilde{\mathbf{H}}_k \mathbf{p}_k \rangle - \langle \mathbf{g}_k, \mathbf{H}_k \mathbf{p}_k \rangle \right)}{L(\mathbf{x}_0) \|\mathbf{p}_k\|^2}. \quad (29)$$

By (10) and Lemmas 3 and 4, we have

$$\begin{aligned} \rho \langle \mathbf{g}_k, \tilde{\mathbf{H}}_k \mathbf{p}_k \rangle - \langle \mathbf{g}_k, \mathbf{H}_k \mathbf{p}_k \rangle &= -(1 - \rho) \langle \mathbf{g}_k, \tilde{\mathbf{H}}_k \mathbf{p}_k \rangle - \langle \mathbf{g}_k, (\mathbf{H}_k - \tilde{\mathbf{H}}_k) \mathbf{p}_k \rangle \\ &\geq (1 - \rho)\tilde{\nu} \|\mathbf{g}_k\|^2 - \frac{\varepsilon}{\tilde{\gamma}} \|\mathbf{g}_k\|^2. \end{aligned}$$

If  $\varepsilon$  satisfies the inequality  $\varepsilon \leq (1 - \rho)\tilde{\nu}\tilde{\gamma}$ , the lower bound on the step-size returned by line-search (27) is  $\alpha_k \geq \alpha$  where

$$\alpha \triangleq \frac{2\tilde{\gamma}^2}{L(\mathbf{x}_0)} \left( (1 - \rho)\tilde{\nu} - \frac{\varepsilon}{\tilde{\gamma}} \right).$$

Otherwise, the lower bound is the trivial  $\alpha = 0$ . Now, from (27) with the lower bound  $\alpha$ , we get

$$\|\mathbf{g}_{k+1}\|^2 \leq \|\mathbf{g}_k\|^2 + 2\rho\alpha_k \langle \tilde{\mathbf{H}}_k \mathbf{p}_k, \mathbf{g}_k \rangle \leq \|\mathbf{g}_k\|^2 - 2\rho\alpha_k \tilde{\nu} \|\mathbf{g}_k\|^2 \leq (1 - 2\rho\alpha\tilde{\nu}) \|\mathbf{g}_k\|^2,$$

which implies  $\eta = 2\rho\alpha\tilde{\nu}$ . We finally note that, from  $\tilde{\nu} \leq \nu$ ,  $\tilde{\gamma} \leq \gamma$ , we have

$$0 \leq \eta = \frac{4\rho\tilde{\nu}\tilde{\gamma}^2}{L(\mathbf{x}_0)} \left( (1 - \rho)\tilde{\nu} - \frac{\varepsilon}{\tilde{\gamma}} \right) \leq \frac{4\rho(1 - \rho)\nu^2\gamma^2}{L(\mathbf{x}_0)} \leq 1,$$

where the second inequality follows from [54, Remark 5].  $\square$

From Theorem 3, it is clear that when  $(1 - \rho)\tilde{\nu} \leq \varepsilon/\tilde{\gamma}$ , we have  $\eta = 0$  and, as a result, a sufficient descent required for convergence cannot be established. This is, in fact, not a by-product of our analysis. Indeed, from Lemma 4, it follows that, as  $\varepsilon \downarrow 0$ , we have  $\tilde{\gamma} \downarrow 0$ , which implies that the least-norm solution can grow unboundedly. This is depicted in Figure 1. As a consequence, the step-size from line-search may shrink to zero to counteract such unbounded growth. This phenomenon is also verified numerically in Section 4.1. However, under certain conditions, we can indeed show that  $\eta > 0$ , which guarantees convergence.

**Corollary 1** (Convergence of Algorithm 1 With Exact Updates Under General Perturbations). *Define*

$$a \triangleq C + 2(1 - \rho), \quad b \triangleq (1 - \rho)(2\nu - 1) - C\sqrt{1 - \nu},$$

$$\delta(t) \triangleq \frac{\sqrt{(t^2 + 4(1 - \rho)^2)^2 - 16(1 - \rho)^4 - (t^2 - 4(1 - \rho)^2)}}{8(1 - \rho)^2} < 1, \quad \forall t \geq 1.$$

*Under the assumptions of Theorem 3, if*

$$\varepsilon < \frac{\gamma \left( 2a + b + 1 - \sqrt{(2a + b + 1)^2 - 8ab} \right)}{4a}, \quad \text{and } \nu > \delta(C),$$

*we have  $\eta \in (0, 1]$ . Here,  $\gamma, \nu, C$  and  $\rho$  are, respectively, as in (6), (8), (15) and (27).*

The proof of Corollary 1 amounts to finding conditions for which  $(1 - \rho)\tilde{\nu} > \varepsilon/\tilde{\gamma}$ , which we omit. However, there is an interesting interplay between  $C$  and  $\nu$  in Corollary 1. Indeed, since  $\delta(t)$  is increasing in  $t$ , for perturbations with large  $C$  in (15), we can guarantee convergence as long as  $\nu$  is close to one, i.e., the gradient contains a very small contribution from  $\text{Null}(\mathbf{H})$ . Furthermore, choosing smaller values for  $\rho$  eases some (though not all) of this restriction on  $\nu$ . However, under inherently stable perturbations (cf. Definition 1), this restriction on  $\nu$  imposed by  $C$  can be entirely removed.

**Corollary 2** (Convergence of Algorithm 1 With Exact Updates Under Inherent Stability). *Under the assumptions of Theorem 3, if the following conditions hold, we have  $\eta \in (0, 1]$ :*

- *if the perturbation is acute and  $\varepsilon$  is small enough such that  $\varepsilon < (1 - \rho)(\gamma - \varepsilon)(\nu\gamma - 2\varepsilon)/\gamma$ , then*

$$\eta \triangleq \frac{4\rho(\nu\gamma - 2\varepsilon)(\gamma - \varepsilon)^2}{\gamma^2 L(\mathbf{x}_0)} \left( (1 - \rho)(\nu\gamma - 2\varepsilon) - \frac{\gamma\varepsilon}{\gamma - \varepsilon} \right) \in (0, 1],$$

- *otherwise if  $\nu = 1$  and  $\varepsilon$  is small enough such that  $\varepsilon < (1 - \rho)(\gamma - \varepsilon)(\gamma - 4\varepsilon)/((1 + 2C)\gamma - 2C\varepsilon)$ , then*

$$\eta \triangleq \frac{4\rho(\gamma - 4\varepsilon)(\gamma - \varepsilon)^2}{((1 + 2C)\gamma - 2C\varepsilon)^2 L(\mathbf{x}_0)} \left( (1 - \rho)(\gamma - 4\varepsilon) - \frac{((1 + 2C)\gamma - 2C\varepsilon)\varepsilon}{\gamma - \varepsilon} \right) \in (0, 1].$$

*Here,  $L(\mathbf{x}_0), \gamma, \nu, C$ , and  $\rho$  are as in (5), (6), (8), (15) and (27), respectively.*

**Remark 2.** For acute perturbations, we see from Corollary 2 that the convergence rate in the limit where  $\varepsilon \downarrow 0$ , matches that of unperturbed algorithm in [54]. For the case where  $\nu = 1$  but the perturbation is not acute, the limiting rate is worse than the unperturbed algorithm, and we believe that this is simply a byproduct of our analysis here.

In the analysis of Newton's method, local convergence rate, i.e., convergence speed in the vicinity of a local solution, plays a critical role. There, by considering  $\alpha_k = 1$ , one can obtain fast problem-independent local convergence rates [55]. Here, we aim to do the same for Algorithm 1. We note

that the notion of “ $\mathbf{x}$  being local” in the context of Newton-MR amounts to “ $\|\mathbf{g}(\mathbf{x})\|$  being small enough” [54]. Obtaining a recursive behavior for  $\|\mathbf{g}\|$  underpins our results here.

**Theorem 4** (Algorithm 1 With  $\alpha_k = 1$  and Exact Updates). *Under the assumptions of Theorem 3 with Assumption 2 replaced with (4b), for the iterates of Algorithm 1 with  $\alpha_k = 1$  and exact update, we have*

$$\|\mathbf{g}(\mathbf{x}_{k+1})\| \leq c_1 \|\mathbf{g}(\mathbf{x}_k)\|^2 + c_2 \|\mathbf{g}(\mathbf{x}_k)\|,$$

where

$$c_1 \triangleq \frac{L_{\mathbf{H}}}{2\tilde{\gamma}^2}, \quad \text{and} \quad c_2 \triangleq \left( \frac{\varepsilon}{\tilde{\gamma}} + \sqrt{1 - \tilde{\nu}} \right)$$

and  $L_{\mathbf{H}}, \tilde{\nu}$  and  $\tilde{\gamma}$  are, respectively, as in (4b) and Lemmas 3 and 4.

*Proof.* With  $\alpha_k = 1$ , we can apply Lemma 3 and the mean-value theorem [22] for vector-valued functions to get

$$\begin{aligned} \|\mathbf{g}(\mathbf{x}_{k+1})\| &= \|\mathbf{g}(\mathbf{x}_k + \mathbf{p}_k)\| = \left\| \mathbf{g}(\mathbf{x}_k) + \int_0^1 \mathbf{H}(\mathbf{x}_k + t\mathbf{p}_k) \mathbf{p}_k dt \right\| \\ &= \left\| \left( \tilde{\mathbf{U}}\tilde{\mathbf{U}}^\top + \tilde{\mathbf{U}}_\perp\tilde{\mathbf{U}}_\perp^\top \right) \mathbf{g}(\mathbf{x}_k) + \int_0^1 \mathbf{H}(\mathbf{x}_k + t\mathbf{p}_k) \mathbf{p}_k dt \right\| \\ &\leq \left\| \tilde{\mathbf{H}}(\mathbf{x}_k)\tilde{\mathbf{H}}^\dagger(\mathbf{x}_k)\mathbf{g}(\mathbf{x}_k) + \int_0^1 \mathbf{H}(\mathbf{x}_k + t\mathbf{p}_k) \mathbf{p}_k dt \right\| + \left\| \tilde{\mathbf{U}}_\perp\tilde{\mathbf{U}}_\perp^\top \mathbf{g}(\mathbf{x}_k) \right\| \\ &\leq \frac{1}{\tilde{\gamma}} \|\mathbf{g}(\mathbf{x}_k)\| \int_0^1 \left\| \mathbf{H}(\mathbf{x}_k + t\mathbf{p}_k) - \tilde{\mathbf{H}}(\mathbf{x}_k) \right\| dt + \sqrt{1 - \tilde{\nu}} \|\mathbf{g}(\mathbf{x}_k)\| \\ &\leq \frac{1}{\tilde{\gamma}} \|\mathbf{g}(\mathbf{x}_k)\| \int_0^1 \left\| \mathbf{H}(\mathbf{x}_k + t\mathbf{p}_k) - \mathbf{H}(\mathbf{x}_k) \right\| dt + \frac{\varepsilon}{\tilde{\gamma}} \|\mathbf{g}(\mathbf{x}_k)\| + \sqrt{1 - \tilde{\nu}} \|\mathbf{g}(\mathbf{x}_k)\| \\ &\leq \frac{L_{\mathbf{H}}}{2\tilde{\gamma}^2} \|\mathbf{g}(\mathbf{x}_k)\|^2 + \left( \frac{\varepsilon}{\tilde{\gamma}} + \sqrt{1 - \tilde{\nu}} \right) \|\mathbf{g}(\mathbf{x}_k)\| \end{aligned}$$

□

Here also as in Theorem 3, unless  $c_2 < 1$ , one cannot establish local convergence using Theorem 4. We now show that for inherently stable perturbations, we can indeed guarantee this. For general perturbations, we note that a similar results as in Corollary 1 can also be obtained in the context of Theorem 4. However, for the sake of simplicity, we opt to omit them here.

**Corollary 3** (Algorithm 1 With  $\alpha_k = 1$  and Exact Updates Under Inherent Stability). *Under the assumptions of Theorem 4, if the following conditions hold, we have  $c_2 < 1$ :*

- if the perturbation is acute and  $\varepsilon$  is small enough such that

$$\varepsilon < (\gamma - \varepsilon) \left( 1 - \sqrt{1 - (\nu - 2\varepsilon/\gamma)} \right),$$

then

$$c_1 = \frac{L_{\mathbf{H}}}{2(\gamma - \varepsilon)^2}, \quad c_2 = \frac{\varepsilon}{(\gamma - \varepsilon)} + \sqrt{1 - \left( \nu - \frac{2\varepsilon}{\gamma} \right)} < 1,$$

- otherwise if  $\nu = 1$  and  $\varepsilon$  is small enough such that

$$\varepsilon < (\gamma - \varepsilon) \left(1 - 2\sqrt{\varepsilon/\gamma}\right) / (1 + 2C),$$

then

$$c_1 = \frac{((1 + 2C)\gamma - 2C\varepsilon)^2 L_{\mathbf{H}}}{2\gamma^2 (\gamma - \varepsilon)^2}, \quad c_2 = \frac{((1 + 2C)\gamma - 2C\varepsilon) \varepsilon}{\gamma (\gamma - \varepsilon)} + 2\sqrt{\frac{\varepsilon}{\gamma}} < 1.$$

Here,  $L_{\mathbf{H}}, \gamma, \nu$  and  $C$  are as in (4b), (7), (8) and (15), respectively.

**Remark 3.** Corollary 3 shows that, under inherent stability and for small  $\varepsilon$ , we obtain a problem-independent local linear convergence rate. For example, consider any  $\varepsilon$  small enough for which we get  $c_2 < 1$ . Then for any  $c_2 < c < 1$ , there exists a  $r > 0$  for which if  $\|\mathbf{g}_k\| \leq r$ , we have  $\|\mathbf{g}_{k+1}\| \leq c \|\mathbf{g}_k\|$ . More generally, however, as  $\varepsilon \downarrow 0$ , since  $\tilde{\gamma} \downarrow 0$ , we can get  $c_2 > 1$  in Theorem 4, which can amount to divergence of the algorithm with constant step-size of  $\alpha_k = 1$ .

### 3.2.2 Inexact Updates

We now turn to convergence analysis of Newton-MR using inexact update (26). Clearly, the inexactness tolerance  $\theta$  has to be chosen with regard to Lemma 3. Indeed, suppose the conditions of Lemma 3 are satisfied. With exact solution to (25), we have

$$\left\langle \mathbf{g}_k, \tilde{\mathbf{H}}_k \mathbf{p}_k + \mathbf{g}_k \right\rangle = - \left\langle \mathbf{g}_k, \tilde{\mathbf{H}}_k \left[ \tilde{\mathbf{H}}_k \right]^\dagger \mathbf{g}_k \right\rangle + \|\mathbf{g}_k\|^2 \leq (1 - \tilde{\nu}) \|\mathbf{g}_k\|^2,$$

where  $\tilde{\nu}$  is defined in Lemma 3. This in turn implies that it is sufficient to choose  $\theta$  such that  $\theta \leq 1 - \tilde{\nu}$ , giving rise to the following condition in inexactness tolerance.

**Condition 2** (Inexactness Tolerance). *The inexactness tolerance,  $\theta$ , in (26) is chosen such that  $1 - \tilde{\nu} \leq \theta < 1$  where  $\tilde{\nu}$  is defined in Lemma 3.*

As advocated in [54], due to several desirable advantages, MINRES-QLP [21] is the method of choice for inexact variant of Newton-MR in which the search direction is computed from (26). Recall that, at the  $k^{\text{th}}$  iteration of Algorithm 1, the  $t^{\text{th}}$  iteration of MINRES-QLP can be represented as

$$\mathbf{p}_k^{(t)} = \arg \min \|\mathbf{p}\|^2, \quad \text{subject to} \quad \mathbf{p} \in \underset{\hat{\mathbf{p}} \in \mathcal{K}_t}{\text{Arg min}} \left\| \tilde{\mathbf{H}}_k \hat{\mathbf{p}} + \mathbf{g}_k \right\|^2, \quad (30)$$

where  $\mathcal{K}_t = \mathcal{K}_t(\tilde{\mathbf{H}}_k, \mathbf{g}_k)$  or  $\mathcal{K}_t = \mathcal{K}_t(\tilde{\mathbf{H}}_k, \tilde{\mathbf{H}}_k \mathbf{g}_k)$ .

Before delving deeper into the analysis of this section, we first give some simple properties of solutions to (26) obtained from MINRES-QLP.

**Lemma 6.** *For any solution to (26) obtained from MINRES-QLP, we have*

$$\left\| \tilde{\mathbf{H}}_k \mathbf{p}_k \right\| \leq \|\mathbf{g}_k\|, \quad (31a)$$

$$\left\| \tilde{\mathbf{H}}_k \mathbf{p}_k + \mathbf{g}_k \right\| \leq \sqrt{\theta} \|\mathbf{g}_k\|. \quad (31b)$$

*Proof.* It has been shown in [21, Lemma 3.3 and Section 6.6] that for  $\mathbf{p}_k^{(t)}$  as in (30),  $\|\tilde{\mathbf{H}}_k \mathbf{p}_k^{(t)}\|$  is monotonically non-decreasing with  $t$ . As a result, we obtain  $\|\tilde{\mathbf{H}}_k \mathbf{p}_k\| \leq \|\tilde{\mathbf{H}}_k \left[ \tilde{\mathbf{H}}_k \right]^\dagger \mathbf{g}_k\| = \|\tilde{\mathbf{U}} \tilde{\mathbf{U}}^\dagger \mathbf{g}_k\| \leq$



$\|\mathbf{g}_k\|$ . Also, from (30) and [21, Lemma 3.3], we always have  $\langle \mathbf{p}_k, \tilde{\mathbf{H}}_k (\tilde{\mathbf{H}}_k \mathbf{p}_k + \mathbf{g}_k) \rangle = 0$ . Now, from (26) we get (31b) as

$$\theta \|\mathbf{g}_k\|^2 \geq \langle \mathbf{g}_k, \tilde{\mathbf{H}}_k \mathbf{p}_k + \mathbf{g}_k \rangle = \langle \mathbf{g}_k, \tilde{\mathbf{H}}_k \mathbf{p}_k + \mathbf{g}_k \rangle + \overbrace{\langle \tilde{\mathbf{H}}_k \mathbf{p}_k, (\tilde{\mathbf{H}}_k \mathbf{p}_k + \mathbf{g}_k) \rangle}^{=0} = \|\tilde{\mathbf{H}}_k \mathbf{p}_k + \mathbf{g}_k\|^2.$$

□

Here, as in Section 3.2.1, establishing the convergence of Algorithm 1 using (26) hinges upon obtaining a bound similar to that in Lemma 4, but in terms of  $\mathbf{p}_k$  from (26). A naïve application of (15) and (31a) gives

$$\|\mathbf{p}_k\| \leq \frac{C}{\varepsilon} \|\tilde{\mathbf{H}}_k \mathbf{p}_k\| \leq \frac{C}{\varepsilon} \|\mathbf{g}_k\|,$$

which implies the search direction can become unbounded as  $\varepsilon \downarrow 0$ . Unfortunately, the norms of the iterates of MINRES-QLP are not necessarily monotonic; see [14, 21, 30]. As a result, although by Lemma 4, we have an upper bound on the final iterate, i.e., the exact solution (24), the intermediate iterates from (30) may have larger norms. Nonetheless, as part of the results of this section, we show that indeed all iterates of MINRES-QLP from (30) are bounded in the same way as in Lemma 4, which can be of independent interest; see Lemma 9.

To achieve this, we first show that (30) can be decoupled into two separate constrained least squares problems. We then show that the solution to each of these least squares problems is indeed bounded.

**Lemma 7.** *For any symmetric matrix  $\mathbf{A} \in \mathbb{R}^{d \times d}$  and  $\mathbf{b} \in \mathbb{R}^d$ , consider the problem*

$$\mathbf{x}^* = \arg \min \|\mathbf{x}\|^2 \quad s.t. \quad \mathbf{x} \in \underset{\hat{\mathbf{x}} \in \mathcal{K}_t}{\text{Arg min}} \|\mathbf{A}\hat{\mathbf{x}} - \mathbf{b}\|^2, \quad (32)$$

where  $\mathcal{K}_t$  is any Krylov subspace. Let  $\mathbf{P}_1$  and  $\mathbf{P}_2$  be orthogonal projectors onto  $\mathbf{A}$ -invariant subspaces. Further, assume that  $\mathbf{P}_1 \mathbf{P}_2 = \mathbf{P}_2 \mathbf{P}_1 = \mathbf{0}$  and  $\text{Range}(\mathbf{A}) = \text{Range}(\mathbf{P}_1) \oplus \text{Range}(\mathbf{P}_2)$ , where  $\oplus$  denotes the direct sum. We have

$$\mathbf{x}^* = \arg \min_{\mathbf{x}_1 \in \mathbf{P}_1 \cdot \mathcal{K}_t} \|\mathbf{A}\mathbf{x}_1 - \mathbf{P}_1 \mathbf{b}\|^2 + \arg \min_{\mathbf{x}_2 \in \mathbf{P}_2 \cdot \mathcal{K}_t} \|\mathbf{A}\mathbf{x}_2 - \mathbf{P}_2 \mathbf{b}\|^2. \quad (33)$$

*Proof.* First note that since  $\mathbf{A}$  is symmetric and  $\mathbf{P}_i, i = 1, 2$ , are the orthogonal projectors onto invariant subspaces of  $\mathbf{A}$ , we have  $\mathbf{P}_i \mathbf{A} = \mathbf{A} \mathbf{P}_i, i = 1, 2$ . Let  $\mathbf{P} = \mathbf{P}_1 + \mathbf{P}_2$ . By Pythagoras theorem we have

$$\|\mathbf{A}\mathbf{x} - \mathbf{b}\|^2 = \|\mathbf{P}\mathbf{A}\mathbf{x} - \mathbf{P}\mathbf{b}\|^2 + \|(\mathbf{I} - \mathbf{P})\mathbf{b}\|^2.$$

Noting that  $\mathbf{x}^* \in \text{Range}(\mathbf{A})$  (see [54, Lemma 7]), we can rewrite (32) as

$$\mathbf{x}^* = \arg \min_{\mathbf{x} \in \mathbf{P} \cdot \mathcal{K}_t} \|\mathbf{A}\mathbf{P}\mathbf{x} - \mathbf{P}\mathbf{b}\|^2.$$

Defining  $\mathbf{x}_i = \mathbf{P}_i \mathbf{x}, i = 1, 2$ , for any  $\mathbf{x} \in \text{Range}(\mathbf{A})$ , we can write  $\mathbf{x} = \mathbf{x}_1 + \mathbf{x}_2$ . Noting that  $\mathbf{P}_1$  and  $\mathbf{P}_2$  are orthogonal projections onto orthogonal subspaces, we have

$$\begin{aligned} \mathbf{x}^* &= \arg \min_{\substack{\mathbf{x}_1 \in \mathbf{P}_1 \cdot \mathcal{K}_t \\ \mathbf{x}_2 \in \mathbf{P}_2 \cdot \mathcal{K}_t}} \|\mathbf{A}(\mathbf{P}_1 \mathbf{x}_1 + \mathbf{P}_2 \mathbf{x}_2) - (\mathbf{P}_1 + \mathbf{P}_2)\mathbf{b}\|^2 \\ &= \arg \min_{\substack{\mathbf{x}_1 \in \mathbf{P}_1 \cdot \mathcal{K}_t \\ \mathbf{x}_2 \in \mathbf{P}_2 \cdot \mathcal{K}_t}} \|\mathbf{P}_1 \mathbf{A}\mathbf{x}_1 + \mathbf{P}_2 \mathbf{A}\mathbf{x}_2 - (\mathbf{P}_1 + \mathbf{P}_2)\mathbf{b}\|^2 \\ &= \arg \min_{\substack{\mathbf{x}_1 \in \mathbf{P}_1 \cdot \mathcal{K}_t \\ \mathbf{x}_2 \in \mathbf{P}_2 \cdot \mathcal{K}_t}} \left( \|\mathbf{P}_1 \mathbf{A}\mathbf{x}_1 - \mathbf{P}_1 \mathbf{b}\|^2 + \|\mathbf{P}_2 \mathbf{A}\mathbf{x}_2 - \mathbf{P}_2 \mathbf{b}\|^2 \right) \\ &= \arg \min_{\mathbf{x}_1 \in \mathbf{P}_1 \cdot \mathcal{K}_t} \|\mathbf{A}\mathbf{x}_1 - \mathbf{P}_1 \mathbf{b}\|^2 + \arg \min_{\mathbf{x}_2 \in \mathbf{P}_2 \cdot \mathcal{K}_t} \|\mathbf{A}\mathbf{x}_2 - \mathbf{P}_2 \mathbf{b}\|^2. \end{aligned}$$

□

The following lemma gives a bound on the solution of each of decoupled terms in (33).

**Lemma 8.** For any symmetric matrix  $\mathbf{A} \in \mathbb{R}^{d \times d}$  and  $\mathbf{b} \in \mathbb{R}^d$ , consider the problem

$$\mathbf{x}^* \triangleq \arg \min_{\mathbf{x} \in \mathbf{P} \cdot \mathcal{K}_t} \|\mathbf{A}\mathbf{x} - \mathbf{P}\mathbf{b}\|, \quad (34)$$

where  $\mathbf{P}$  is the orthogonal projector onto a  $\mathbf{A}$ -invariant subspace and  $\mathcal{K}_t$  is  $\mathcal{K}_t(\mathbf{A}, \mathbf{b})$  or  $\mathcal{K}_t(\mathbf{A}, \mathbf{A}\mathbf{b})$ , for  $t \in \{1, 2, \dots, \text{Rank}(\mathbf{A}\mathbf{P})\}$ . We have

$$\|\mathbf{x}^*\| \leq \|\mathbf{P}\mathbf{b}\| \left\| [\mathbf{A}\mathbf{P}]^\dagger \right\|.$$

*Proof.* Clearly, we can replace (34) with an equivalent formulation as

$$\mathbf{x}^* = \arg \min_{\mathbf{x} \in \mathbf{P} \cdot \mathcal{K}_t} \|\mathbf{A}\mathbf{P}\mathbf{x} - \mathbf{P}\mathbf{b}\|.$$

We prove the result for when  $\mathcal{K}_t = \mathcal{K}_t(\mathbf{A}, \mathbf{b})$  as the case of  $\mathcal{K}_t = \mathcal{K}_t(\mathbf{A}, \mathbf{A}\mathbf{b})$  is proven similarly. As before, since  $\mathbf{A}$  is symmetric and  $\mathbf{P}$  is the orthogonal projector onto an invariant subspace of  $\mathbf{A}$ , we have  $\mathbf{P}\mathbf{A} = \mathbf{A}\mathbf{P}$ , hence  $\mathbf{A}\mathbf{P}$  is also symmetric. Consider applying Lanczos process to obtain the decomposition

$$\mathbf{A}\mathbf{P}\mathbf{Q}_t = \mathbf{Q}_{t+1}\mathbf{T}_t,$$

where  $\mathbf{T}_t \in \mathbb{R}^{(t+1) \times t}$  and  $\mathbf{Q}_t = [\mathbf{q}_1, \mathbf{q}_2, \dots, \mathbf{q}_t]$  is an orthonormal basis for the Krylov subspace  $\mathbf{P} \cdot \mathcal{K}_t = \mathcal{K}_t(\mathbf{A}\mathbf{P}, \mathbf{P}\mathbf{b})$  and  $\mathbf{Q}_{t+1} = [\mathbf{Q}_t \mid \mathbf{q}_{t+1}]$  with  $\mathbf{Q}_{t+1}^\top \mathbf{q}_{t+1} = \mathbf{0}$ . Recall that one can find  $\mathbf{x}^* = \mathbf{Q}_t \mathbf{y}^*$  where

$$\mathbf{y}^* \triangleq \arg \min_{\mathbf{y} \in \mathbb{R}^t} \|\mathbf{T}_t \mathbf{y} - \mathbf{Q}_{t+1}^\top \mathbf{P}\mathbf{b}\|.$$

It follows that

$$\|\mathbf{x}^*\| = \|\mathbf{Q}_t \mathbf{y}^*\| = \|\mathbf{y}^*\| = \left\| \mathbf{T}_t^\dagger \mathbf{Q}_{t+1}^\top \mathbf{P}\mathbf{b} \right\|.$$

Also, we have

$$\left\| \mathbf{T}_t^\dagger \right\| = \left\| [\mathbf{Q}_{t+1} \mathbf{T}_t \mathbf{Q}_t^\top]^\dagger \right\| \leq \left\| [\mathbf{Q}_{t+2} \mathbf{T}_{t+1} \mathbf{Q}_{t+1}^\top]^\dagger \right\| \leq \dots \leq \left\| [\mathbf{A}\mathbf{P}]^\dagger \right\|,$$

where the first equality is obtained by noting that

$$[\mathbf{Q}_{t+1} \mathbf{T}_t \mathbf{Q}_t^\top]^\dagger = [\mathbf{T}_t \mathbf{Q}_t^\top]^\dagger [\mathbf{Q}_{t+1}]^\top = \mathbf{Q}_t \mathbf{T}_t^\dagger \mathbf{Q}_{t+1}^\top,$$

and the series of inequalities follow from [13, Proposition 2.1]. So, we finally get

$$\|\mathbf{x}^*\| = \left\| \mathbf{T}_t^\dagger \mathbf{Q}_{t+1}^\top \mathbf{P}\mathbf{b} \right\| \leq \|\mathbf{P}\mathbf{b}\| \left\| \mathbf{T}_t^\dagger \right\| \leq \|\mathbf{P}\mathbf{b}\| \left\| [\mathbf{A}\mathbf{P}]^\dagger \right\|.$$

□

We are now ready to prove a result similar to Lemma 4 for the case of inexact updates.

**Lemma 9.** Under Assumptions of Lemma 4, for the iterates of MINRES-QLP in (30), we have

$$\left\| \mathbf{p}_k^{(t)} \right\| \leq \frac{1}{\tilde{\gamma}} \|\mathbf{g}_k\|, \quad t = 1, 2, \dots, \text{Rank}(\tilde{\mathbf{H}}_k),$$

where  $\tilde{\gamma}$  is as in Lemma 4.

*Proof.* For simplicity, we drop the dependence on  $k$  and  $t$ . Let  $\tilde{\mathbf{P}}_1, \tilde{\mathbf{P}}_2$  and  $\tilde{\mathbf{P}}_\perp$  denote the projectors  $\tilde{\mathbf{U}}_1\tilde{\mathbf{U}}_1^\top, \tilde{\mathbf{U}}_2\tilde{\mathbf{U}}_2^\top$  and  $\tilde{\mathbf{U}}_\perp\tilde{\mathbf{U}}_\perp^\top$ , respectively, where  $\tilde{\mathbf{U}}_1, \tilde{\mathbf{U}}_2$  and  $\tilde{\mathbf{U}}_\perp$  are defined in (22). Also, let  $\tilde{\mathbf{P}} = \tilde{\mathbf{P}}_1 + \tilde{\mathbf{P}}_2$ . Using Lemma 7, we can write (30) as  $\mathbf{p} = \mathbf{p}_1 + \mathbf{p}_2$ , where

$$\mathbf{p}_1 = \arg \min_{\mathbf{p} \in \tilde{\mathbf{P}}_1 \cdot \mathcal{K}_t} \left\| \tilde{\mathbf{H}}\mathbf{p} + \tilde{\mathbf{P}}_1\mathbf{g} \right\|, \quad \mathbf{p}_2 = \arg \min_{\mathbf{p} \in \tilde{\mathbf{P}}_2 \cdot \mathcal{K}_t} \left\| \tilde{\mathbf{H}}\mathbf{p} + \tilde{\mathbf{P}}_2\mathbf{g} \right\|.$$

From Lemma 8 and (20), it follows that

$$\|\mathbf{p}_1\| \leq \left\| \tilde{\mathbf{P}}_1\mathbf{g} \right\| \left\| \left[ \tilde{\mathbf{H}}\tilde{\mathbf{P}}_1 \right]^\dagger \right\| = \left\| \tilde{\mathbf{U}}_1\tilde{\mathbf{U}}_1^\top\mathbf{g} \right\| \left\| \left[ \tilde{\mathbf{U}}_1\tilde{\mathbf{U}}_1^\top\tilde{\mathbf{H}} \right]^\dagger \right\| \leq \frac{1}{\gamma - \varepsilon} \|\mathbf{g}\|.$$

Similarly, by (9b), (21), Theorem 1, and Lemma 8, we have

$$\begin{aligned} \|\mathbf{p}_2\| &\leq \left\| \tilde{\mathbf{P}}_2\mathbf{g} \right\| \left\| \left[ \tilde{\mathbf{H}}\tilde{\mathbf{P}}_2 \right]^\dagger \right\| \leq \left\| \left( \tilde{\mathbf{U}}_2\tilde{\mathbf{U}}_2^\top + \tilde{\mathbf{U}}_\perp\tilde{\mathbf{U}}_\perp^\top \right) \mathbf{g} \right\| \left\| \left[ \tilde{\mathbf{U}}_2\tilde{\mathbf{U}}_2^\top\tilde{\mathbf{H}} \right]^\dagger \right\| \\ &\leq \frac{C}{\varepsilon} \left\| \left( \tilde{\mathbf{U}}_2\tilde{\mathbf{U}}_2^\top + \tilde{\mathbf{U}}_\perp\tilde{\mathbf{U}}_\perp^\top - \mathbf{U}_\perp\mathbf{U}_\perp^\top + \mathbf{U}_\perp\mathbf{U}_\perp^\top \right) \mathbf{g} \right\| \\ &\leq \frac{C}{\varepsilon} \left\| \left( \mathbf{U}\mathbf{U}^\top - \tilde{\mathbf{U}}_1\tilde{\mathbf{U}}_1^\top + \mathbf{U}_\perp\mathbf{U}_\perp^\top \right) \mathbf{g} \right\| \leq \frac{C}{\varepsilon} \left( \frac{2\varepsilon}{\gamma} + \sqrt{1-\nu} \right) \|\mathbf{g}\|, \end{aligned}$$

which gives us

$$\|\mathbf{p}_2\| \leq C \left( \frac{2}{\gamma} + \frac{\sqrt{1-\nu}}{\varepsilon} \right) \|\mathbf{g}\|.$$

Finally, we obtain

$$\|\mathbf{p}\|^2 = \|\mathbf{p}_1 + \mathbf{p}_2\|^2 = \|\mathbf{p}_1\|^2 + \|\mathbf{p}_2\|^2 \leq \left( \left( \frac{1}{\gamma - \varepsilon} \right)^2 + \left( C \left( \frac{2}{\gamma} + \frac{\sqrt{1-\nu}}{\varepsilon} \right) \right)^2 \right) \|\mathbf{g}\|^2.$$

The result follows from the inequality  $\sqrt{a^2 + b^2} \leq a + b, \forall a, b \geq 0$ .  $\square$

The inexactness condition in (26) involves two criteria for an approximate solution  $\mathbf{p}_k$ , namely feasibility of  $\mathbf{p}_k$  in (26) and that  $\mathbf{p}_k \in \text{Range}(\tilde{\mathbf{H}}_k)$ . When  $\mathbf{g}_k \in \text{Range}(\tilde{\mathbf{H}}_k)$ , the latter is enforced naturally as a result of MINRES-QLP's underlying Krylov subspace. However, in cases where  $\mathbf{g}_k \notin \text{Range}(\tilde{\mathbf{H}}_k)$ , one could simply modify the Krylov subspace as described in [54]. To allow for unification of the results of this section, we define *range-invariant* Krylov subspace, which encapsulate these variants.

**Definition 2** (Range-invariant Krylov Subspace). *For any symmetric matrix  $\mathbf{A}$ , the range-invariant Krylov subspace is defined as follows.*

(i) *If  $\mathbf{b} \in \text{Range}(\mathbf{A})$ , we can consider the usual  $\mathcal{K}_t(\mathbf{A}, \mathbf{b})$ , e.g., MINRES [51].*

(ii) *Otherwise, we can always employ  $\mathcal{K}_t(\mathbf{A}, \mathbf{A}\mathbf{b})$ , e.g., MR-II [36].*

*Here,  $t = 1, \dots, \text{Rank}(\mathbf{A})$ .*

In the subsequent discussion, we always assume that MINRES-QLP used within Algorithm 1 generates iterates from an appropriate range-invariant Krylov subspace,  $\mathcal{K}_t(\tilde{\mathbf{H}}_k, \mathbf{g}_k)$  or  $\mathcal{K}_t(\tilde{\mathbf{H}}_k, \tilde{\mathbf{H}}_k\mathbf{g}_k)$  (cf. (30)).

Now, similar with the proofs for exact updates Theorem 3, we can obtain the following results for Algorithm 1 with inexact updates satisfying (26).

**Theorem 5** (Algorithm 1 With Inexact Updates). *Under Assumptions 1 to 5 and Conditions 1 and 2, for the iterates of Algorithm 1 with inexact updates, we have*

$$\|\mathbf{g}_{k+1}\|^2 \leq (1 - \eta) \|\mathbf{g}_k\|^2$$

where

$$\eta \triangleq \max \left\{ 0, \frac{4\rho\tilde{\gamma}^2(1-\theta)}{L(\mathbf{x}_0)} \left( (1-\rho)(1-\theta) - \frac{\varepsilon}{\tilde{\gamma}} \right) \right\} \in [0, 1],$$

and  $\rho, L(\mathbf{x}_0), \tilde{\nu}, \tilde{\gamma}$  and  $\theta$  are, respectively, as in (27), Assumption 2, Lemmas 3 and 4, and Condition 2.

*Proof.* Similar with the proof for Theorem 3, by (10) and (26) and Lemma 9, we have

$$\begin{aligned} \rho \langle \mathbf{g}_k, \tilde{\mathbf{H}}_k \mathbf{p}_k \rangle - \langle \mathbf{g}_k, \mathbf{H}_k \mathbf{p}_k \rangle &= -(1-\rho) \langle \mathbf{g}_k, \tilde{\mathbf{H}}_k \mathbf{p}_k \rangle + \langle \mathbf{g}_k, (\tilde{\mathbf{H}}_k - \mathbf{H}_k) \mathbf{p}_k \rangle \\ &\geq (1-\rho)(1-\theta) \|\mathbf{g}_k\|^2 - \frac{\varepsilon}{\tilde{\gamma}} \|\mathbf{g}_k\|^2. \end{aligned}$$

If  $\varepsilon$  satisfies the inequality  $\varepsilon \leq (1-\rho)(1-\theta)\tilde{\gamma}$ , the lower bound on the step-size returned by line-search (27) is  $\alpha_k \geq \alpha$  where

$$\alpha \triangleq \frac{2\tilde{\gamma}^2}{L(\mathbf{x}_0)} \left( (1-\rho)(1-\theta) - \frac{\varepsilon}{\tilde{\gamma}} \right).$$

Otherwise, the lower bound is the trivial  $\alpha = 0$ . Now, from (27) with the lower bound  $\alpha$ , we get

$$\|\mathbf{g}_{k+1}\|^2 \leq \|\mathbf{g}_k\|^2 + 2\rho\alpha_k \langle \tilde{\mathbf{H}}_k \mathbf{p}_k, \mathbf{g}_k \rangle \leq \|\mathbf{g}_k\|^2 - 2\rho\alpha_k(1-\theta) \|\mathbf{g}_k\|^2 \leq (1 - 2\rho\alpha(1-\theta)) \|\mathbf{g}_k\|^2,$$

which implies  $\eta = 2\rho\alpha(1-\theta)$ . We finally note since  $(1-\theta) \leq \tilde{\nu}$ , similarly to the line of reasoning at the end of the proof of Theorem 3, we can deduce that  $\eta \in [0, 1]$ .  $\square$

**Remark 4.** Note that when  $\theta = 1 - \tilde{\nu}$ , Theorems 3 and 5 exactly coincide.

From Theorem 5, similar to Theorem 3, one cannot establish sufficient descent required for convergence unless  $\eta > 0$ . However, similar results as those of Corollaries 1 and 2 corresponding to Theorem 5 can also be easily established here. We omit those results for the sake of brevity. Nonetheless, the interesting interplay between  $\varepsilon$  and  $\theta$  that arises as a result of Theorem 5 should be highlighted. For example, suppose  $\nu = 1$ . By inspecting the condition  $\eta > 0$ , i.e.,  $\varepsilon < \tilde{\gamma}(1-\rho)(1-\theta)$ , one can see that the smaller values of  $\varepsilon$ , i.e., more accurate estimations of  $\mathbf{H}$ , allow for larger values of  $\theta$ , which, in turn, amount to cruder approximations to the exact least-norm solution. In other words, Hessian approximation and sub-problem accuracy in the form of least-squares residual (cf. (31b)) are inversely related.

As in Theorem 4, we can obtain a recursive behavior of  $\|\mathbf{g}_k\|$  for the case where  $\alpha_k = 1$ , which can then be used to deduce a local problem-independent convergence rate similar to that described in Remark 3.

**Theorem 6** (Algorithm 1 With  $\alpha_k = 1$  and Inexact Updates). *Under the assumptions of Theorem 5 with Assumption 2 replaced with (4b), for the iterates of Algorithm 1 with  $\alpha_k = 1$  and inexact updates (26), we have*

$$\|\mathbf{g}(\mathbf{x}_{k+1})\| \leq \frac{L_{\mathbf{H}}}{2\tilde{\gamma}^2} \|\mathbf{g}(\mathbf{x}_k)\|^2 + \left( \frac{\varepsilon}{\tilde{\gamma}} + \sqrt{\theta} \right) \|\mathbf{g}(\mathbf{x}_k)\|.$$

where  $L_{\mathbf{H}}, \tilde{\gamma}$  and  $\theta$  are, respectively, as in (4b), Lemma 4, and Condition 2.

*Proof.* Similarly to the proof of Theorem 4, using (31b), we have

$$\begin{aligned}
\|\mathbf{g}(\mathbf{x}_{k+1})\| &= \|\mathbf{g}(\mathbf{x}_k + \mathbf{p}_k)\| = \left\| \mathbf{g}(\mathbf{x}_k) + \int_0^1 \mathbf{H}(\mathbf{x}_k + t\mathbf{p}_k) \mathbf{p}_k dt \right\| \\
&= \left\| \mathbf{g}(\mathbf{x}_k) + \tilde{\mathbf{H}}(\mathbf{x}_k) \mathbf{p}_k - \tilde{\mathbf{H}}(\mathbf{x}_k) \mathbf{p}_k + \int_0^1 \mathbf{H}(\mathbf{x}_k + t\mathbf{p}_k) \mathbf{p}_k dt \right\| \\
&\leq \left\| -\tilde{\mathbf{H}}(\mathbf{x}_k) \mathbf{p}_k + \int_0^1 \mathbf{H}(\mathbf{x}_k + t\mathbf{p}_k) \mathbf{p}_k dt \right\| + \left\| \mathbf{g}(\mathbf{x}_k) + \tilde{\mathbf{H}}(\mathbf{x}_k) \mathbf{p}_k \right\| \\
&\leq \|\mathbf{p}_k\| \int_0^1 \|\mathbf{H}(\mathbf{x}_k + t\mathbf{p}_k) - \mathbf{H}(\mathbf{x}_k)\| dt + \varepsilon \|\mathbf{p}_k\| + \sqrt{\theta} \|\mathbf{g}(\mathbf{x}_k)\| \\
&\leq \frac{L_{\mathbf{H}}}{2\tilde{\gamma}^2} \|\mathbf{g}(\mathbf{x}_k)\|^2 + \left( \frac{\varepsilon}{\tilde{\gamma}} + \sqrt{\theta} \right) \|\mathbf{g}(\mathbf{x}_k)\|.
\end{aligned}$$

□

**Remark 5.** Here also, when  $\theta = 1 - \tilde{\nu}$ , Theorems 4 and 6 exactly coincide.

Just as in Section 3.2.1, with some simple algebraic manipulations, we can easily derive sufficient conditions on  $\varepsilon$  such that  $\varepsilon/\tilde{\gamma} + \sqrt{\theta} < 1$  in Theorem 6 (for example a similar result to Corollary 3 in the special case of inherently-stable perturbations). We omit those results for the sake of brevity.

### 3.3 Comparison with Sub-sampled Newton Method

As mentioned in Section 1, even though Newton-MR can be readily applied, beyond strongly-convex settings, to the more general class of invex problems, its iterations bear a strong resemblance to those of the classical Newton's algorithm. Hence, it is illuminating to have a renewed look at the results of this paper in light of the existing results on Newton's method (and its Newton-CG variant) in the contexts of inexact Hessian and strong convexity. To do this, we consider the setting of finite-sum minimization problem (2) and compare the present results with those of [55]. For concreteness, we consider [55, Theorem 13], which gives the global convergence of sub-sampled Newton method with problem-independent local convergence rate. To create a level playing field here, we make the same assumptions as those of [55, Theorem 13], namely each  $f_i$  is twice-differentiable, smooth and convex, i.e.,  $0 \leq \lambda_{\min}(\mathbf{H}_i(\mathbf{x})) \leq \lambda_{\max}(\mathbf{H}_i(\mathbf{x})) \leq L_i$ ,  $\forall \mathbf{x} \in \mathbb{R}^d$  where  $\mathbf{H}_i(\mathbf{x}) \triangleq \nabla^2 f_i(\mathbf{x})$ ,  $f$  is  $\gamma$ -strongly convex with Lipschitz gradient and Hessian, i.e., it satisfies (4). Note that by [54, Lemma 1], we have that  $L(\mathbf{x}_0) = L_{\mathbf{g}}^2 + L_{\mathbf{H}} \|\nabla f(\mathbf{x}_0)\|$  where  $L(\mathbf{x}_0)$  is as in (5). As in [55, Section 1.5], we define  $\kappa \triangleq L_{\mathbf{g}}/\gamma$  and  $\kappa_{\max} \triangleq \max_i L_i/\gamma$  as the problem and sub-sampling condition numbers, respectively. Note that  $\kappa_{\max} \geq \kappa$ . We also define  $\kappa_0 \triangleq \sqrt{L(\mathbf{x}_0)}/\gamma$ . Now, by the assumption on  $\varepsilon$  in [55, Theorem 13], we have  $\varepsilon \in \mathcal{O}(1/\sqrt{\kappa_{\max}})$ , which in light of [55, Lemma 2] implies that a sample size of  $|\mathcal{S}| \in \tilde{\mathcal{O}}(\kappa_{\max}^2)$  guarantees (11).

Specialized to strongly-convex problems, from Lemma 2, we have that  $\text{Rank}(\mathbf{H}) = \text{Rank}(\tilde{\mathbf{H}}) = d$ , which implies  $\tilde{\nu} = 1$  and also gives  $\tilde{\gamma} = \gamma - \varepsilon$  in Lemma 4. Now, from Theorem 3, we get

$$\eta = \frac{4\rho(\gamma - \varepsilon)^2}{L_{\mathbf{g}}^2 + L_{\mathbf{H}} \|\nabla f(\mathbf{x}_0)\|} \left( (1 - \rho) - \frac{\varepsilon}{\gamma - \varepsilon} \right).$$

Choosing  $\varepsilon \leq (1 - \rho)\gamma/(2 - \rho)$  implies  $\eta \geq 8\rho(1 - \rho)/(3 - \rho)^2 \kappa_0^2$ . With this  $\varepsilon$ , [67, Lemma 16] implies that a sample size of  $|\mathcal{S}| \in \tilde{\mathcal{O}}(\kappa_{\max}^2)$  is required to form  $\tilde{\mathbf{H}}$ , which is of the same order as that for sub-sampled Newton's method above. Similarly, with this  $\varepsilon$ , the local convergence result of Theorem 4 can be stated with  $c_2 \leq (1 - \rho)/2$ . For inexact update in Section 3.2.2, we can also derive similar results in the present context. Here, we emphasize that since  $\tilde{\nu} = 1$ , the inexactness tolerance can be

set to any value  $\theta \in [0, 1)$  in Condition 2. This is in sharp contrast to sub-sampled Newton-CG in which the inexactness tolerance is of the order  $\theta \in \mathcal{O}(1/\sqrt{\kappa_{\max}})$ , which is rather restrictive; see [55] for further details on inexactness tolerance for sub-sampled Newton-CG.

We put all this together in Table 1. We also convert the convergence results of this paper in  $\|\mathbf{g}\|$  to those of [55] which are in terms of  $f - f^*$  and  $\|\mathbf{x} - \mathbf{x}^*\|$  for global and local convergence regimes, respectively. For this we use the well-known facts about strong convexity [47] that

$$\|\mathbf{g}(\mathbf{x})\| \geq \gamma \|\mathbf{x} - \mathbf{x}^*\|, \quad \text{and} \quad \|\mathbf{g}(\mathbf{x})\|^2 \geq 2\gamma(f(\mathbf{x}) - f(\mathbf{x}^*)).$$

In evaluating the complexities, we have assumed that the cost of one Hessian-vector product is of the same order as evaluating a gradient, e.g, [35, 52, 55, 69]. From Table 1, the overall worst-case running-time of an algorithm to achieve the prescribed sub-optimality is estimated as  $(nd + \text{Column \#2} \times \text{Column \#3}) \times (\text{Column \#4 or Column \#5})$ , the first term  $nd$  is the cost of evaluating the full gradient.

Table 1: Complexity comparison of variants of Newton’s method and Newton-MR methods for (2). The notation  $\tilde{\mathcal{O}}$  implies hidden logarithmic factors, e.g.,  $\ln(\kappa), \ln(\kappa_{\max}), \ln(d)$ . Constants  $\gamma, \kappa, \kappa_{\max}, \kappa_0$  are defined in Section 3.3. Fourth column gathers iteration complexity to achieve sub-optimality  $f(\mathbf{x}_k) - f(\mathbf{x}^*) \leq \varsigma$  for some  $\varsigma \leq 1$ . Fifth column reflect the corresponding complexity to achieve  $\|\mathbf{x}_k - \mathbf{x}^*\| \leq \varsigma$  for some  $\varsigma \leq 1$ , assuming  $\mathbf{x}_0$  is close enough to  $\mathbf{x}^*$ .

Method	Evaluating Hessian-Vector Product, $\mathbf{H}\mathbf{v}$	# of Iterations of MIN-RES/CG	Global Iteration Complexity	Local Iteration Complexity	Reference
Newton	$\mathcal{O}(nd)$	$\mathcal{O}(d)$	$\mathcal{O}(\kappa^2 \ln \frac{1}{\varsigma})$	$\mathcal{O}(\ln \ln \frac{1}{\varsigma})$	Folklore
Newton-CG	$\mathcal{O}(nd)$	$\tilde{\mathcal{O}}(\sqrt{\kappa})$	$\mathcal{O}(\kappa^2 \ln \frac{1}{\varsigma})$	$\mathcal{O}(\ln \frac{1}{\varsigma})$	Folklore
Sub-sampled Newton	$\tilde{\mathcal{O}}(d\kappa_{\max}^2)$	$\mathcal{O}(d)$	$\mathcal{O}(\kappa\kappa_{\max} \ln \frac{1}{\varsigma})$	$\mathcal{O}(\ln \frac{1}{\varsigma})$	[55, Theorem 13]
Sub-sampled Newton-CG	$\tilde{\mathcal{O}}(d\kappa_{\max}^2)$	$\tilde{\mathcal{O}}(\sqrt{\kappa_{\max}})$	$\mathcal{O}(\kappa\kappa_{\max} \ln \frac{1}{\varsigma})$	$\mathcal{O}(\ln \frac{1}{\varsigma})$	[55, Theorem 13]
Newton-MR (Exact Update)	$\tilde{\mathcal{O}}(nd)$	$\mathcal{O}(d)$	$\mathcal{O}(\kappa_0^2 \ln \frac{1}{\varsigma})$	$\mathcal{O}(\ln \ln \frac{1}{\varsigma})$	[54, Corollary 1, Theorem 2]
Newton-MR (Inexact Update)	$\tilde{\mathcal{O}}(nd)$	$\tilde{\mathcal{O}}(\sqrt{\kappa})$	$\mathcal{O}(\kappa_0^2 \ln \frac{1}{\varsigma})$	$\mathcal{O}(\ln \frac{1}{\varsigma})$	[54, Corollary 2, Theorem 4]
Algorithm 1 with (25)	$\tilde{\mathcal{O}}(d\kappa_{\max}^2)$	$\mathcal{O}(d)$	$\mathcal{O}(\kappa_0^2 \ln \frac{1}{\varsigma})$	$\mathcal{O}(\ln \frac{1}{\varsigma})$	Theorems 3 and 4
Algorithm 1 with (26)	$\tilde{\mathcal{O}}(d\kappa_{\max}^2)$	$\tilde{\mathcal{O}}(\sqrt{\kappa_{\max}})$	$\mathcal{O}(\kappa_0^2 \ln \frac{1}{\varsigma})$	$\mathcal{O}(\ln \frac{1}{\varsigma})$	Theorems 5 and 6

Table 1 gives complexities involved in various algorithms for achieving sub-optimality in objective value, i.e.,  $f(\mathbf{x}_k) - f(\mathbf{x}^*) \leq \varsigma$  for some  $\varsigma \leq 1$  and the corresponding complexity to achieve  $\|\mathbf{x}_k - \mathbf{x}^*\| \leq \varsigma$  for some  $\varsigma \leq 1$ , assuming  $\mathbf{x}_0$  is in the vicinity of the solution  $\mathbf{x}^*$ . We note that the complexities given in Table 1 are , not only, for worst-case analysis, but also they are pessimistic. For example, from the worst-case complexity of the algorithms with Hessian sub-sampling, it appears that they are advantageous only in some marginal cases. However, this is unfortunately a side-effect of our analysis and not an inherent property of the sub-sampled algorithm. In this light, any conclusions from these tables should be made with great care.

In the strongly-convex setting with the above smoothness assumptions, since  $\kappa_0 \geq \kappa$ , the global worst-case iteration complexity of Newton-MR is worse than that of Newton-CG (of course, Newton-MR applies to the larger class of invex objectives, which are also allowed to be less smooth than what is assumed to generate Table 1; see [54] for a detailed discussion.) However, for sub-sampled variants of these algorithms, the comparison is not as straightforward. Indeed, the interplay between  $\mathbf{x}_0, L_{\mathbf{H}}$ , and  $\max_i L_i$  determines the relationship between  $\kappa\kappa_{\max}$  and  $\kappa_0^2$ . For examples, if  $\mathbf{x}_0$  is chosen such that  $\|\nabla f(\mathbf{x}_0)\| \ll 1$ , then one expects to see  $\kappa_0^2 \leq \kappa\kappa_{\max}$ , which implies Algorithm 1 should perform

better than sub-sampled Newton methods in [55]. Similarly, if  $L_i$ 's are very non-uniform, then noting that  $L_{\mathbf{g}} \leq \sum_{i=1}^n L_i/n$ , we can also expect  $\kappa_{\max} \gg \kappa$ , which could imply  $\kappa_0^2 \leq \kappa\kappa_{\max}$ .

Although not reflected in Table 1, it has been shown that for linear systems involving positive definite systems, MINRES can achieve a given relative residual tolerance in far fewer iterations than CG; see [30] for a detailed discussion. This observation indicates that Algorithm 1 with (26) should typically converge faster than sub-sampled Newton-CG method of [55]. This is indeed confirmed by the numerical experiments of Section 4. Finally, from Table 1, we can also see that in the absence of a good preconditioner, if  $\kappa_{\max} \geq d^2$ , solving (25) exactly can be potentially more efficient than resorting to an inexact method.

## 4 Numerical Experiments

In this section, we empirically verify the theoretical results of this paper and also evaluate the performance of Newton-MR as compared with several optimization methods. In particular, we first study the effect of unstable perturbations with  $\nu < 1$  in Section 4.1 and show that, somewhat unintuitively, reducing the perturbations indeed results in worsening of the performance. In Section 4.2, we then turn our attention to two class of problems where  $\nu = 1$  and demonstrate that such inherent stability allows for the design of a highly efficient variant of Newton-MR in which the Hessian is approximated. The code for the experiments is available at <https://github.com/syangliu/Newton-MR>.

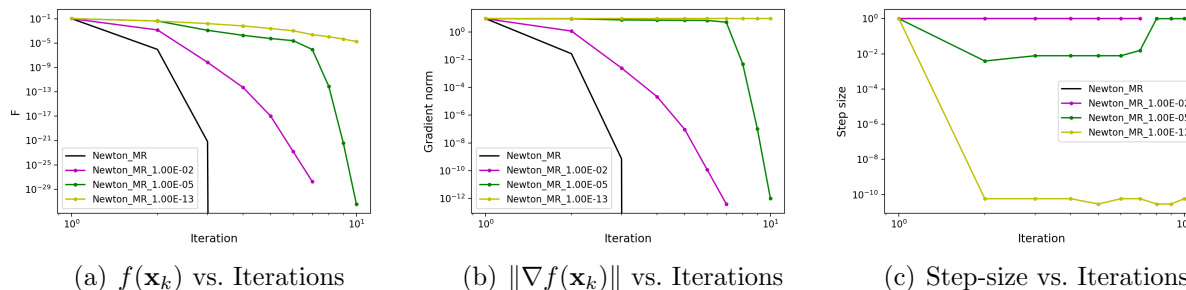


Figure 2: Performance of Newton-MR under an unstable perturbation for  $\varepsilon = 10^{-2}$ ,  $10^{-5}$ , and  $10^{-13}$  as in Section 4.1, e.g., “Newton-MR\_1.00E-02” refers to the perturbation with  $\varepsilon = 10^{-2}$ . “Newton-MR” refers to unperturbed algorithm.

### 4.1 Unstable Perturbations

We now verify the theoretical results of this paper in case of unstable perturbations where  $\nu < 1$  and the perturbation is not acute. For this, we consider a simple two dimensional function, taken from [54, Example 5], as

$$f(x_1, x_2) = \frac{ax_1^2}{b - x_2}, \quad (35)$$

where  $\text{dom}(f) = \{(x_1, x_2) \mid x_1 \in \mathbb{R}, x_2 \in (-\infty, b) \cup (b, \infty)\}$ . Clearly,  $f$  is unbounded below and, admittedly, this example is of little interest in optimization. In fact, applying Algorithm 1 to (35) amounts to finding its stationary points, which are of the form  $(0, x_2) \in \text{dom}(f)$ . Nonetheless, (35) serves our purpose of demonstrating the effects of unstable perturbations in the performance of Algorithm 1.

In [54, Example 5], it has been shown that  $\nu = 8/9$ . Here, we consider  $a = 100, b = 1$  and  $\mathbf{x}_0$  is chosen randomly from standard normal distribution. We draw a symmetric random matrix  $\mathbf{E}$  from the Gaussian orthogonal ensemble and form the perturbed Hessian as  $\tilde{\mathbf{H}} = \mathbf{H} + \varepsilon\mathbf{E}/\|\mathbf{E}\|$ . We consider Algorithm 1 with exact updates for unperturbed as well as perturbed Hessian with  $\varepsilon = 10^{-2}$ ,  $10^{-5}$ , and

2nd-order Methods	Newton-MR	Newton-CG	Gauss-Newton	ssNewton-MR	ssNewton-CG	L-BFGS
	$2(t + \ell + 1)$	$2t + \ell + 2$	$2t + \ell + 2$	$2ts/n + 2(\ell + 1)$	$2ts/n + \ell + 2$	$2(\ell + 1)$
1st-order Methods	Momentum	Adagrad	Adadelta	RMSprop	Adam	SGD
	$2b/n$	$2b/n$	$2b/n$	$2b/n$	$2b/n$	$2b/n$

Table 2: Complexity measure for each iteration of the algorithms for a finite-sum minimization problem involving  $n$  functions. Sub-sampled variants of Newton-MR and Newton-CG are referred to, respectively as “ssNewton-MR” and “ssNewton-CG”. We also use  $t$  and  $\ell$  to denote, respectively, the total number of iterations for the corresponding inner solver and the line-search. The sample size for estimating the Hessian is denoted by  $s$ , whereas  $b$  refers the mini-batch size for first-order methods.

$10^{-13}$ , respectively. As seen in Figure 2, for such an unstable perturbation, better approximations to the true Hessian, perhaps unintuitively, do not necessarily help with the convergence. In fact, smaller values of  $\varepsilon$  amount to search directions that grow unboundedly larger, which result in the step-size shrinking to zero to counteract such unbounded growth; see Figure 1 for a depiction of this phenomenon. These numerical observations reaffirm the theoretical results of Section 3.2.

## 4.2 Stable Perturbations

In this section, we demonstrate the efficiency of Algorithm 1 under inherently stable perturbations. Our empirical evaluations of this section are done in the context of finite-sum minimization (2). We first make comparisons among several Newton-type methods. In particular, we consider Newton-MR, Newton-CG, as well as their stochastic variants in which the Hessian matrix is sub-sampled, while the function and its gradient are computed exactly. We also consider the classical Gauss-Newton as well as L-BFGS. We then turn our attention to comparison among sub-sampled Newton-MR and several first-order alternatives, namely SGD with and without momentum [64], Adagrad [28], RMSProp [65], Adam [39], and Adadelta [71]. We consider both deterministic and stochastic variants of the first-order algorithms where the gradient is, respectively, computed exactly and estimated using sub-samples. All first-order algorithms in this section use constant step-sizes, which are carefully fine-tuned for each experiment to give the best performance in terms of reducing the objective value.

**Complexity Measure** In all of our experiments, in addition to “wall-clock” time, we consider total number of oracle calls of function, gradient and Hessian-vector product as a complexity measure for evaluating the performance of each algorithm. Similar to [54, Section 4], this is a judicious decision as measuring “wall-clock” time can be highly affected by particular implementation details. More specifically, for each  $i$  in (2), after computing  $f_i(\mathbf{x})$ , computing  $\nabla f_i(\mathbf{x})$  is equivalent to one additional function evaluation. In our implementations, we merely require Hessian-vector products  $\nabla^2 f_i(\mathbf{x})\mathbf{v}$ , instead of forming the explicit Hessian, which amounts to two additional function evaluations, as compared with gradient evaluation. The number of such oracle calls for all algorithms considered here is given in Table 2.

**Parameters** Throughout this section, we set the maximum iterations of the underlying inner solver, e.g., MINRES-QLP or CG, to 200 with an inexact tolerance of  $\theta = 10^{-2}$ . In Algorithm 1, for the termination criterion and the Armijo line-search parameter, respectively, we set  $\tau = 10^{-10}$  and  $\rho = 10^{-4}$ . Both Newton-CG and Gauss-Newton use the standard Armijo line-search whose parameter is also set to  $\rho = 10^{-4}$ . The parameter of the strong Wolfe curvature condition, used for L-BFGS, is 0.4. The history size of L-BFGS will be kept at 20 past iterations. In the rest of this section, all methods are always initialized at  $\mathbf{x}_0 = \mathbf{0}$ . For Newton-type methods, the initial trial step-size in line-search is always taken to be one.



### 4.2.1 Softmax regression

Here, we consider the softmax cross-entropy minimization problem without regularization. More specifically, we have

$$f(\mathbf{x}) \triangleq \mathcal{L}(\mathbf{x}_1, \mathbf{x}_2, \dots, \mathbf{x}_{C-1}) = \sum_{i=1}^n \left( \log \left( 1 + \sum_{c'=1}^{C-1} e^{\langle \mathbf{a}_i, \mathbf{x}_{c'} \rangle} \right) - \sum_{c=1}^{C-1} \mathbf{1}(b_i = c) \langle \mathbf{a}_i, \mathbf{x}_c \rangle \right), \quad (36)$$

where  $\{\mathbf{a}_i, b_i\}_{i=1}^n$  with  $\mathbf{a}_i \in \mathbb{R}^p$ ,  $b_i \in \{0, 1, \dots, C\}$  denote the training data,  $C$  is the total number of classes for each input data  $\mathbf{a}_i$  and  $\mathbf{x} = (\mathbf{x}_1, \mathbf{x}_2, \dots, \mathbf{x}_{C-1})$ . Note that, in this case, we have  $d = (C-1) \times p$ . It can be shown that, depending on the data, (36) is either strictly-convex or merely weakly-convex. In either case, however, it has been shown in [54] that  $\nu = 1$ , i.e.,  $\nabla f(\mathbf{x}_k) \in \text{Range}(\nabla^2 f(\mathbf{x}_k))$ .

Figure 3, 4 and 5 depict, respectively, the performance of variants of Newton-MR as compared with other Newton-type methods and several (stochastic) first-order methods. As it can be seen, all variants of Newton-MR are not only highly efficient in terms of oracle calls, but also they are very competitive in terms of “wall-clock” time. In fact, we can see that sub-sampled Newton-MR converges faster than all first-order methods. This can be attributed to moderate per-iteration cost of sub-sampled Newton-MR, which is coupled with far fewer overall iterations.

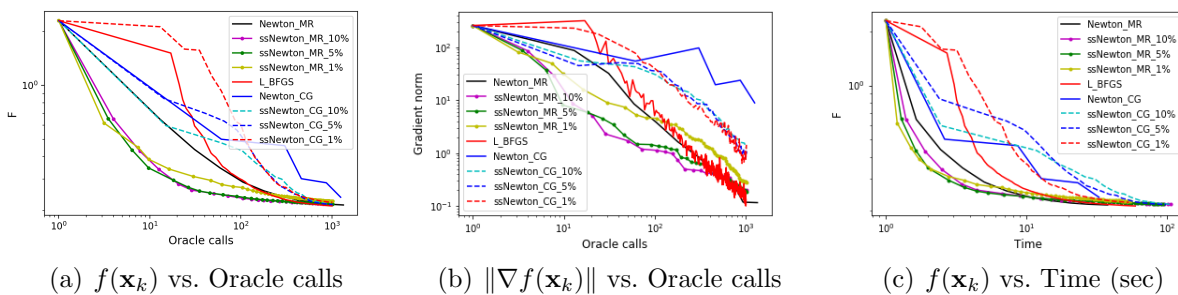


Figure 3: Comparison among Newton-type methods on (36) using MNIST dataset. Here, sample sizes are chosen as  $s = 0.1n, 0.05n$  and  $0.01n$ , e.g., “ssNewton-MR\_10%” uses  $s = 0.1n$ .

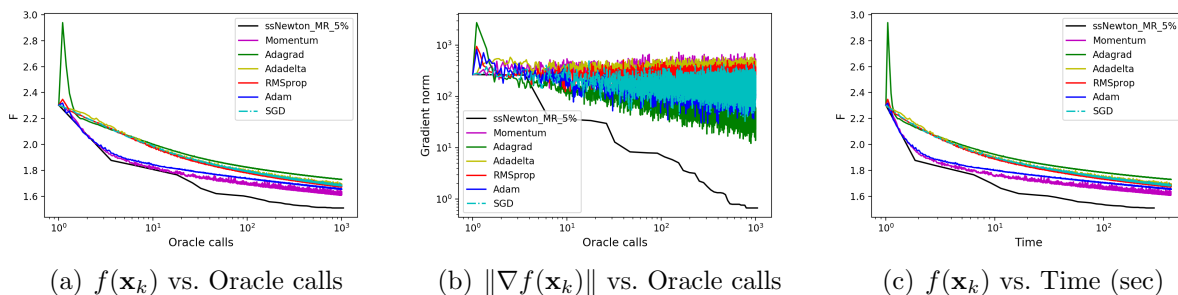


Figure 4: Comparison among sub-sampled Newton-MR and several first-order methods on (36) using Cifar10 dataset. Here, sample/mini-batch sizes are  $s = b = 0.05n$ .

We then compare the performance of Newton-MR and Newton-CG as it relates to sensitivity to Hessian perturbations. We consider full and sub-sampled variants of both algorithms for a range of sample-sizes. Figures 6 and 7 clearly demonstrate that Newton-MR exhibits a great deal of robustness to Hessian perturbations, which amount to better performance for crude Hessian approximations. This is in sharp contrast to Newton-CG, which requires more accurate Hessian estimations to perform comparatively. Note the large variability in the performance of sub-sampled Newton-CG as compared with rather uniform performance of sub-sampled Newton-MR.

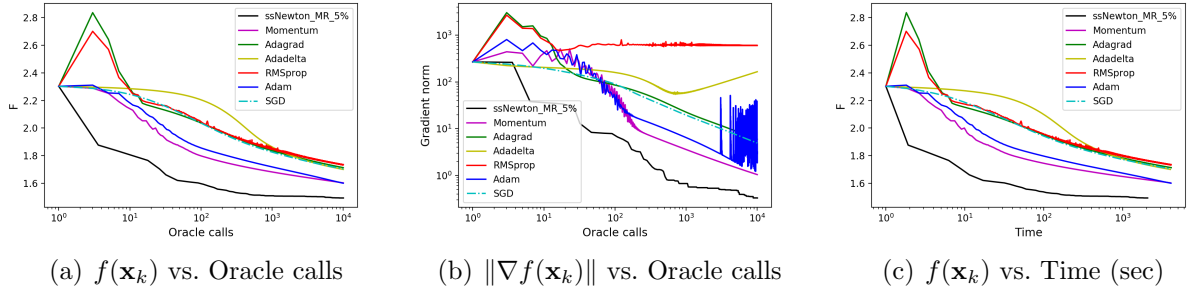


Figure 5: Comparison among sub-sampled Newton-MR and several first-order methods on (36) using Cifar10 dataset. Here, sample/mini-batch sizes are  $s = 0.05n$ ,  $b = n$ .

## 4.2.2 Gaussian Mixture Model

Here, we consider an example involving a mixture of Gaussian densities. Although this problem is non-convex, it exhibits features that are close to being convex, e.g, small regions of saddle points and large regions containing global minimum [44]. For simplicity, we consider a mixture model with two Gaussian components as

$$f(\mathbf{x}) \triangleq \mathcal{L}(w, \mathbf{u}, \mathbf{v}) = - \sum_{i=1}^n \log (\zeta(w) \Phi(\mathbf{a}_i; \mathbf{u}, \Sigma_1) + (1 - \zeta(w)) \Phi(\mathbf{a}_i; \mathbf{v}, \Sigma_2)), \quad (37)$$

where  $\Phi$  denotes the density of the  $p$ -dimensional standard normal distribution,  $\mathbf{a}_i \in \mathbb{R}^p$  are the data points,  $\mathbf{u}, \mathbf{v} \in \mathbb{R}^p$ ,  $\Sigma_1, \Sigma_2 \in \mathbb{R}^{p \times p}$  are the corresponding mean vectors and the covariance matrices of two Gaussian distributions,  $w \in \mathbb{R}$  and  $\zeta(t) = 1/(1+e^{-t})$  is to ensure that the mixing weight lies within  $[0, 1]$ . Here, one can show that  $\nu = 1$ . Note that, here,  $\mathbf{x} \triangleq [w; \mathbf{u}; \mathbf{v}] \in \mathbb{R}^{2p+1}$ . In each run, we generate 1,000 random data points, generated from the mixture distribution (37) with  $p = 100$ , and ground truth parameters as  $w^* \sim \mathcal{N}[0, 1]$ ,  $\mathbf{u}^* \sim \mathcal{N}[-1, 1]$ ,  $\mathbf{v}^* \sim \mathcal{U}[3, 4]$ . Covariance matrices are constructed randomly, with controlled condition number, such that they are not axis-aligned. To establish this, we first randomly generate two  $p \times p$  matrices whose elements are i.i.d. drawn from standard normal distribution and uniform distribution, respectively. We then find the corresponding orthogonal bases,  $\mathbf{Q}_1, \mathbf{Q}_2$ , using QR factorization. We then set  $\Sigma_i = \mathbf{Q}_i^T \mathbf{D}^{-1} \mathbf{Q}_i$  where  $\mathbf{D}$  is a diagonal matrix whose diagonal entries are chosen equidistantly from the interval  $[0, 10^8]$ . This way the condition number of each  $\Sigma_i$  is  $10^8$ . In all the figures,

$$\text{Estimation error at } k^{\text{th}} \text{ iteration} \triangleq \frac{1}{2} \left( \frac{|w_k - w^*|}{w^*} + \frac{\|[\mathbf{u}_k; \mathbf{v}_k] - [\mathbf{u}^*; \mathbf{v}^*]\|}{\|[\mathbf{u}^*; \mathbf{v}^*]\|} \right).$$

In our experiments, the classical Gauss-Newton method performed extremely poorly, and as a result we did not consider its sub-sampled variants. Figure 8 shows the performance profile plots [27, 33] with 500 runs for Newton-type methods and Figures 9 and 10 depict the corresponding plots comparing variants of Newton-MR with several first-order methods using, respectively, sample/mini-batch sizes of 5% and the full gradient. Recall that in performance profile plots, for a given  $\lambda$  in the x-axis, the corresponding value on the y-axis is the proportion of times that a given solver's performance lies within a factor  $\lambda$  of the best possible performance over all runs.

As demonstrated by Figure 8, although L-BFGS performs competitively in terms of reducing the objective function, its performance in terms of parameter recovery and estimation error is far worse than all other methods. In contrast, all variants of Newton-MR have stable performance across all 500 runs, with sub-sampled variants exhibiting superior performance. Figure 9 and 10 also demonstrate similar superior performance compared with first-order algorithms.

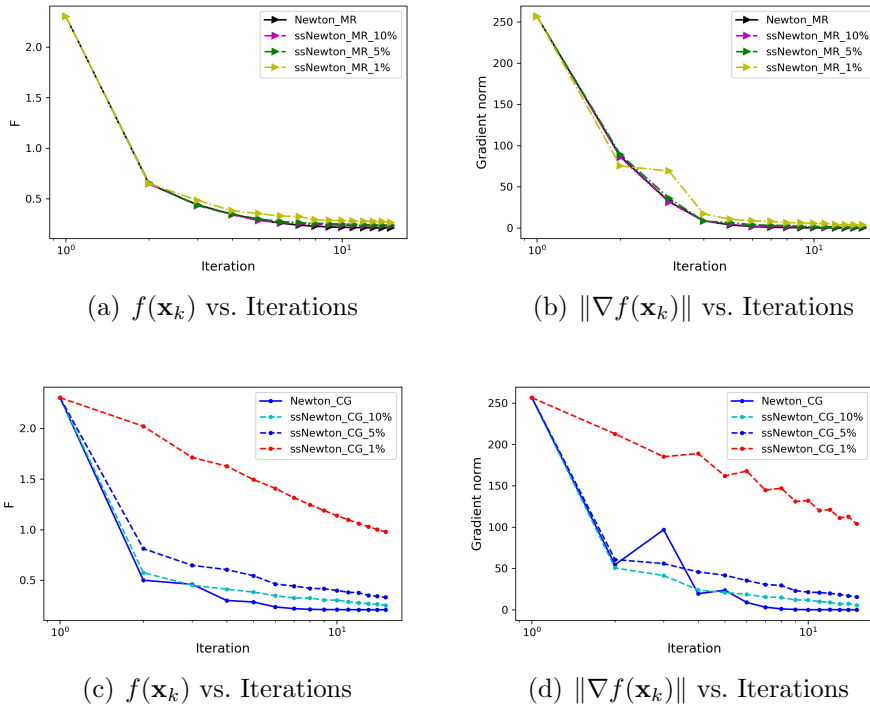


Figure 6: Stability comparison between full and sub-sampled variants of Newton-MR and Newton-CG using  $s = 0.1n, 0.05n, 0.01n$  in Table 2 on (36) with MNIST dataset.

## 5 Conclusions

We considered the convergence analysis of Newton-MR [54] under inexact Hessian information in the form of additive noise perturbations. It is known that the pseudo-inverse of the Hessian is a discontinuous function of such perturbations. As a result, the pseudo-inverse of the perturbed Hessian can grow unboundedly with diminishing noise. However, our results indicate that it can indeed remain bounded along certain directions and under favorable conditions. We showed that the concept of inherently stable perturbations encapsulates situations under which Newton-MR with noisy Hessian remains stably convergent. Under such conditions, we established global and local convergence results for Algorithm 1 using both exact and inexact updates. We argued that such stability analysis allows for the design of efficient variants of Newton-MR in which Hessian is approximated to reduce the computational costs in large-scale problems. We then numerically demonstrated the validity of our theoretical result and evaluated the performance of several such variants of Newton-MR as compared with various first and second-order methods.

## Acknowledgment

All authors are grateful for the support by the Australian Centre of Excellence for Mathematical and Statistical Frontiers (ACEMS). Fred Roosta was partially supported by DARPA D3M as well as the Australian Research Council through a Discovery Early Career Researcher Award (DE180100923).

## References

- [1] Andrew J Ballard, Ritankar Das, Stefano Martiniani, Dhagash Mehta, Levent Sagun, Jacob D Stevenson, and David J Wales. Energy landscapes for machine learning. *Physical Chemistry Chemical Physics*, 19(20):12585–12603, 2017.

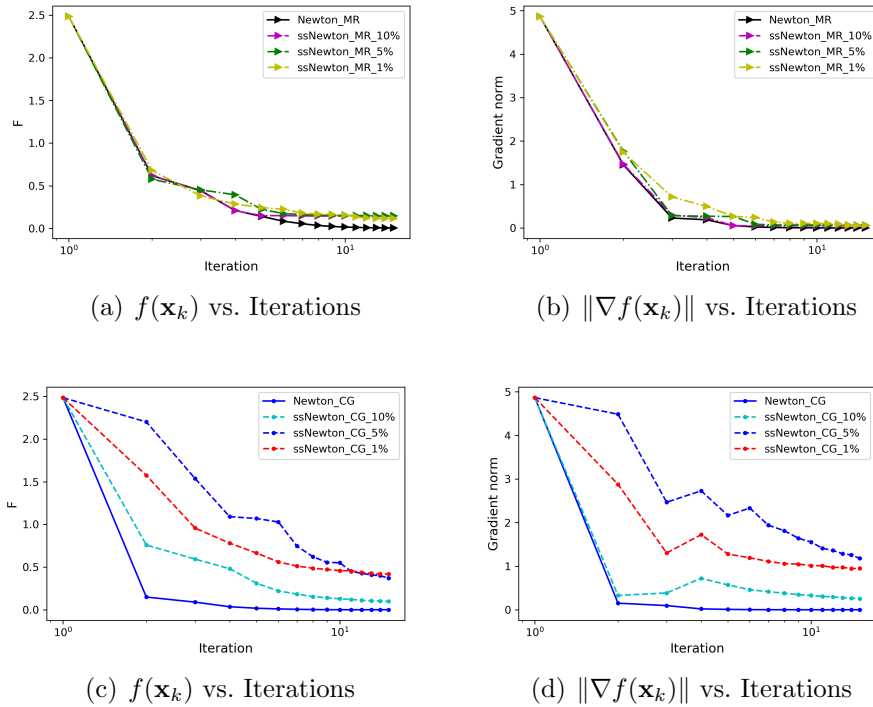


Figure 7: Stability comparison between full and sub-sampled variants of Newton-MR and Newton-CG using  $s = 0.1n, 0.05n, 0.01n$  in Table 2 on (36) with HAPT dataset.

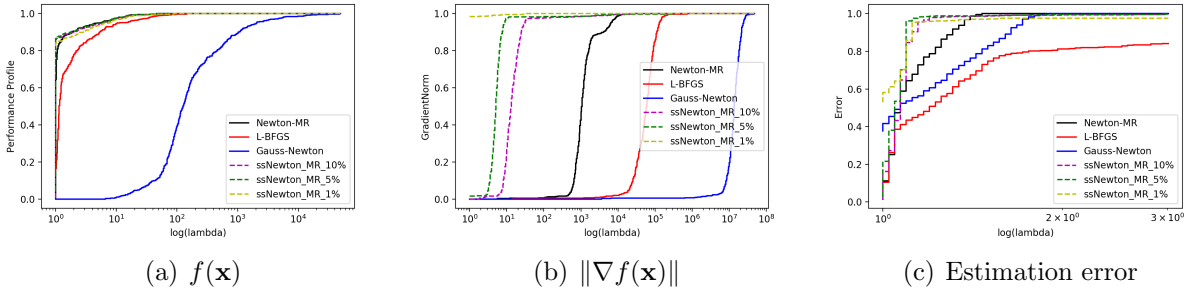


Figure 8: Performance profile for 500 runs of various Newton-type methods for solving (37) as detailed in Section 4.2.2.

- [2] Afonso S Bandeira, Katya Scheinberg, and Luís N Vicente. Convergence of trust-region methods based on probabilistic models. *SIAM Journal on Optimization*, 24(3):1238–1264, 2014.
- [3] A Ben-Israel and B Mond. What is invexity? *The ANZIAM Journal*, 28(1):1–9, 1986.
- [4] Albert S Berahas, Raghu Bollapragada, and Jorge Nocedal. An investigation of Newton-sketch and subsampled Newton methods. *arXiv preprint arXiv:1705.06211*, 2017.
- [5] Dennis S Bernstein. *Matrix Mathematics: Theory, Facts, and Formulas With Application to Linear Systems Theory*, volume 41. Princeton University Press Princeton, 2009.
- [6] Dimitri P. Bertsekas. *Convex Optimization Algorithms*. Athena Scientific Belmont, 2015.
- [7] Jose Blanchet, Coralia Cartis, Matt Menickelly, and Katya Scheinberg. Convergence rate analysis of a stochastic trust region method for nonconvex optimization. *arXiv preprint arXiv:1609.07428*, 2016.
- [8] Raghu Bollapragada, Richard H Byrd, and Jorge Nocedal. Exact and inexact subsampled Newton methods for optimization. *IMA Journal of Numerical Analysis*, 39(2):545–578, 2019.

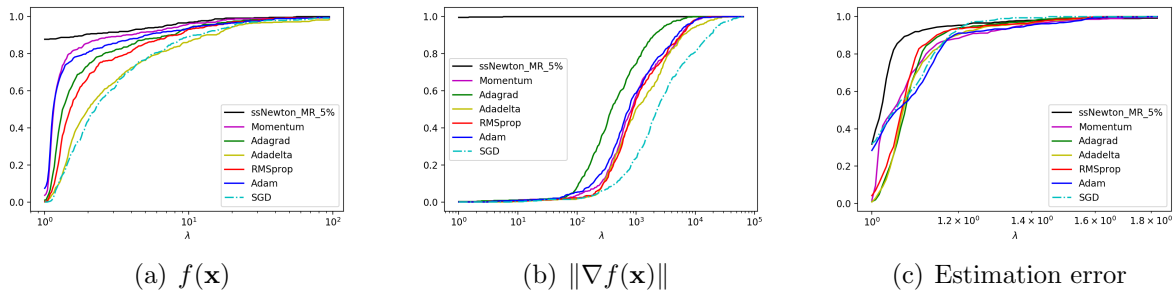


Figure 9: Performance profile for 500 runs of Newton-MR variants and several first-order methods for solving (37) as detailed in Section 4.2.2. Here, we have set  $s = b = 0.05n$ .

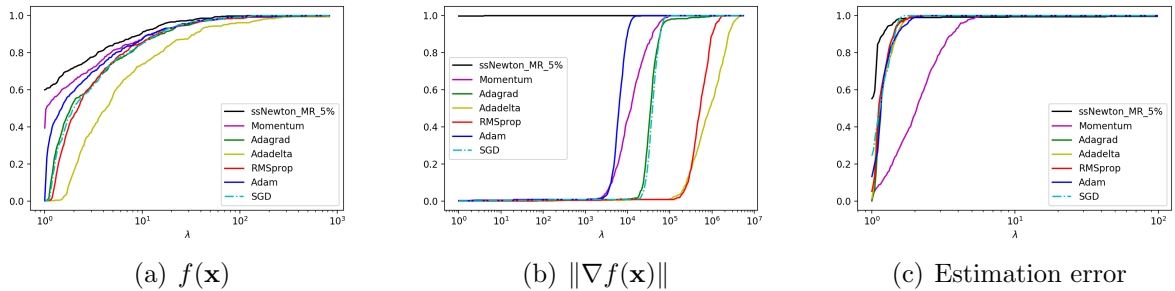


Figure 10: Performance profile for 500 runs of Newton-MR variants and several first-order methods for solving (37) as detailed in Section 4.2.2. Here, we have set  $s = 0.05n$ ,  $b = n$ .

- [9] Stephen Boyd and Lieven Vandenbergh. *Convex optimization*. Cambridge university press, 2004.
- [10] Richard H. Byrd, Gillian M. Chin, Will Neveitt, and Jorge Nocedal. On the use of stochastic Hessian information in optimization methods for machine learning. *SIAM Journal on Optimization*, 21(3):977–995, 2011.
- [11] Richard H. Byrd, Gillian M. Chin, Jorge Nocedal, and Yuchen Wu. Sample size selection in optimization methods for machine learning. *Mathematical programming*, 134(1):127–155, 2012.
- [12] Richard H Byrd, Humaid Fayez Khalfan, and Robert B Schnabel. Analysis of a symmetric rank-one trust region method. *SIAM Journal on Optimization*, 6(4):1025–1039, 1996.
- [13] D Calvetti, B Lewis, and L Reichel. GMRES, L-curves, and discrete ill-posed problems. *BIT Numerical Mathematics*, 42(1):44–65, 2002.
- [14] Daniela Calvetti, Bryan Lewis, and Lothar Reichel. L-curve for the MINRES method. In *Advanced Signal Processing Algorithms, Architectures, and Implementations X*, volume 4116, pages 385–396. International Society for Optics and Photonics, 2000.
- [15] Yair Carmon, John C Duchi, Oliver Hinder, and Aaron Sidford. Convex until proven guilty: Dimension-free acceleration of gradient descent on non-convex functions. In *Proceedings of the 34th International Conference on Machine Learning-Volume 70*, pages 654–663. JMLR. org, 2017.
- [16] Yair Carmon, John C Duchi, Oliver Hinder, and Aaron Sidford. Accelerated methods for non-convex optimization. *SIAM Journal on Optimization*, 28(2):1751–1772, 2018.
- [17] C Cartis, N. I. M. Gould, and Philip L. Toint. Adaptive cubic regularisation methods for unconstrained optimization. Part I: motivation, convergence and numerical results. *Mathematical Programming*, 127(2):245–295, 2011.
- [18] C Cartis, N. I. M. Gould, and Philip L. Toint. Adaptive cubic regularisation methods for unconstrained optimization. Part II: worst-case function-and derivative-evaluation complexity. *Mathematical programming*, 130(2):295–319, 2011.

- [19] Coralia Cartis, N. I. M. Gould, and Philip L. Toint. Complexity bounds for second-order optimality in unconstrained optimization. *Journal of Complexity*, 28(1):93–108, 2012.
- [20] Ruobing Chen, Matt Menickelly, and Katya Scheinberg. Stochastic optimization using a trust-region method and random models. *Mathematical Programming*, 169(2):447–487, 2018.
- [21] Sou-Cheng T Choi, Christopher C Paige, and Michael A Saunders. MINRES-QLP: A Krylov subspace method for indefinite or singular symmetric systems. *SIAM Journal on Scientific Computing*, 33(4):1810–1836, 2011.
- [22] P.G. Ciarlet. *Linear and Nonlinear Functional Analysis with Applications*. SIAM, 2013.
- [23] Andrew R Conn, N. I. M. Gould, and Philip L. Toint. *Trust region methods*, volume 1. SIAM, 2000.
- [24] Andrew R Conn, Nicholas IM Gould, and Ph L Toint. Convergence of quasi-Newton matrices generated by the symmetric rank one update. *Mathematical programming*, 50(1-3):177–195, 1991.
- [25] CY Deng and Yimin Wei. Perturbation analysis of the Moore-Penrose inverse for a class of bounded operators in Hilbert spaces. *J. Korean Math. Soc.*, 47(4):831–843, 2010.
- [26] John E Dennis Jr and Robert B Schnabel. *Numerical methods for unconstrained optimization and nonlinear equations*. SIAM, 1996.
- [27] Elizabeth D Dolan and Jorge J Moré. Benchmarking optimization software with performance profiles. *Mathematical programming*, 91(2):201–213, 2002.
- [28] John Duchi, Elad Hazan, and Yoram Singer. Adaptive subgradient methods for online learning and stochastic optimization. *The Journal of Machine Learning Research*, 12:2121–2159, 2011.
- [29] Murat A. Erdogdu and Andrea Montanari. Convergence rates of sub-sampled Newton methods. In *Advances in Neural Information Processing Systems 28*, pages 3034–3042. 2015.
- [30] David Chin-Lung Fong and Michael Saunders. CG versus MINRES: An empirical comparison. *Sultan Qaboos University Journal for Science [SQUJS]*, 17(1):44–62, 2012.
- [31] Charles G Frye, Neha S Wadia, Michael R DeWeese, and Kristofer E Bouchard. Numerically recovering the critical points of a deep linear autoencoder. *arXiv preprint arXiv:1901.10603*, 2019.
- [32] G.H. Golub and C.F. Van Loan. *Matrix Computations*. Johns Hopkins Studies in the Mathematical Sciences. Johns Hopkins University Press, 4 edition, 2012.
- [33] Nicholas Gould and Jennifer Scott. A note on performance profiles for benchmarking software. *ACM Transactions on Mathematical Software (TOMS)*, 43(2):15, 2016.
- [34] Gratton, Serge and Royer, Clément W and Vicente, Luís N and Zhang, Zaikun. Complexity and global rates of trust-region methods based on probabilistic models. *IMA Journal of Numerical Analysis*, 38(3):1579–1597, 2018.
- [35] Andreas Griewank. Some bounds on the complexity of gradients, Jacobians, and Hessians. *Complexity in Nonlinear Optimization*, pages 128–161, 1993.
- [36] Martin Hanke. *Conjugate gradient type methods for ill-posed problems*. Routledge, 2017.
- [37] Morgan A Hanson. On sufficiency of the Kuhn-Tucker conditions. *Journal of Mathematical Analysis and Applications*, 80(2):545–550, 1981.
- [38] John H Hubbard and Barbara Burke Hubbard. *Vector Calculus, Linear Algebra, and Differential Forms*. Matrix Editions, 5th edition, 2015.
- [39] Diederik Kingma and Jimmy Ba. Adam: A method for stochastic optimization. *arXiv preprint arXiv:1412.6980*, 2014.
- [40] Sudhir Kylasa, Fred Roosta, Michael W Mahoney, and Ananth Grama. GPU Accelerated Sub-Sampled Newton’s Method for Convex Classification Problems. In *Proceedings of the 2019 SIAM International Conference on Data Mining*, pages 702–710. SIAM, 2019.

- [41] Jeffrey Larson and Stephen C Billups. Stochastic derivative-free optimization using a trust region framework. *Computational Optimization and Applications*, 64(3):619–645, 2016.
- [42] Kenneth Levenberg. A method for the solution of certain problems in least squares. *Quarterly of Applied Mathematics*, 2(2):164–168, 1944.
- [43] Donald W Marquardt. An algorithm for least-squares estimation of nonlinear parameters. *Journal of the Society for Industrial & Applied Mathematics*, 11(2):431–441, 1963.
- [44] Song Mei, Yu Bai, and Andrea Montanari. The landscape of empirical risk for non-convex losses. *arXiv preprint arXiv:1607.06534*, 2016.
- [45] Lingsheng Meng and Bing Zheng. The optimal perturbation bounds of the Moore–Penrose inverse under the Frobenius norm. *Linear Algebra and its Applications*, 432(4):956–963, 2010.
- [46] Shashi K Mishra and Giorgio Giorgi. *Invecity and Optimization*, volume 88. Springer Science & Business Media, 2008.
- [47] Yurii Nesterov. *Introductory lectures on convex optimization*, volume 87. Springer Science & Business Media, 2004.
- [48] Yurii Nesterov and Boris T Polyak. Cubic regularization of Newton method and its global performance. *Mathematical Programming*, 108(1):177–205, 2006.
- [49] Jorge Nocedal and Stephen Wright. *Numerical optimization*. Springer Science & Business Media, 2006.
- [50] Sean O’Rourke, Van Vu, and Ke Wang. Random perturbation of low rank matrices: Improving classical bounds. *Linear Algebra and its Applications*, 540:26–59, 2018.
- [51] Christopher C Paige and Michael A Saunders. Solution of sparse indefinite systems of linear equations. *SIAM journal on numerical analysis*, 12(4):617–629, 1975.
- [52] Barak A Pearlmutter. Fast exact multiplication by the Hessian. *Neural computation*, 6(1):147–160, 1994.
- [53] Mert Pilanci and Martin J. Wainwright. Newton Sketch: A Linear-time Optimization Algorithm with Linear-Quadratic Convergence. *arXiv preprint arXiv:1505.02250*, 2015.
- [54] Fred Roosta, Yang Liu, Peng Xu, and Michael W Mahoney. Newton-MR: Newton’s Method Without Smoothness or Convexity. *arXiv preprint arXiv:1810.00303*, 2018.
- [55] Fred Roosta and Michael W. Mahoney. Sub-sampled Newton methods. *Mathematical Programming*, 174(1):293–326, 2019.
- [56] Fred Roosta, Kees van den Doel, and Uri Ascher. Stochastic algorithms for inverse problems involving PDEs and many measurements. *SIAM J. Scientific Computing*, 36(5):S3–S22, 2014.
- [57] Clément W Royer, Michael O’Neill, and Stephen J Wright. A newton-cg algorithm with complexity guarantees for smooth unconstrained optimization. *Mathematical Programming*, 180(1):451–488, 2020.
- [58] Clément W Royer and Stephen J Wright. Complexity analysis of second-order line-search algorithms for smooth nonconvex optimization. *SIAM Journal on Optimization*, 28(2):1448–1477, 2018.
- [59] Mark Rudelson and Roman Vershynin. Non-asymptotic theory of random matrices: extreme singular values. In *Proceedings of the International Congress of Mathematicians 2010 (ICM 2010) (In 4 Volumes) Vol. I: Plenary Lectures and Ceremonies Vols. II–IV: Invited Lectures*, pages 1576–1602. World Scientific, 2010.
- [60] Shai Shalev-Shwartz and Shai Ben-David. *Understanding machine learning: From theory to algorithms*. Cambridge university press, 2014.
- [61] Sara Shashaani, Fatemeh S Hashemi, and Raghu Pasupathy. ASTRO-DF: A class of adaptive sampling trust-region algorithms for derivative-free stochastic optimization. *SIAM Journal on Optimization*, 28(4):3145–3176, 2018.

- [62] GW Stewart. Rank degeneracy. *SIAM Journal on Scientific and Statistical Computing*, 5(2):403–413, 1984.
- [63] G.W. Stewart and Ji guang Sun. *Matrix Perturbation Theory*. Academic Press, 1990.
- [64] Ilya Sutskever, James Martens, George Dahl, and Geoffrey Hinton. On the importance of initialization and momentum in deep learning. In *International conference on machine learning*, pages 1139–1147, 2013.
- [65] Tijmen Tieleman and Geoffrey Hinton. Lecture 6.5-rmsprop: Divide the gradient by a running average of its recent magnitude. *COURSERA: Neural Networks for Machine Learning*, 4, 2012.
- [66] David Wales et al. *Energy landscapes: Applications to clusters, biomolecules and glasses*. Cambridge University Press, 2003.
- [67] Peng Xu, Fred Roosta, and Michael W Mahoney. Newton-type methods for non-convex optimization under inexact Hessian information. *Mathematical Programming*, 2019. doi:10.1007/s10107-019-01405-z.
- [68] Peng Xu, Fred Roosta, and Michael W Mahoney. Second-order optimization for non-convex machine learning: An empirical study. In *Proceedings of the 2020 SIAM International Conference on Data Mining*, pages 199–207. SIAM, 2020.
- [69] Peng Xu, Jiyan Yang, Fred Roosta, Christopher Ré, and Michael W Mahoney. Sub-sampled newton methods with non-uniform sampling. In *Advances in Neural Information Processing Systems*, pages 3000–3008, 2016.
- [70] Zhewei Yao, Peng Xu, Fred Roosta, and Michael W Mahoney. Inexact non-convex Newton-type methods. *arXiv preprint arXiv:1802.06925*, 2018.
- [71] Matthew D Zeiler. ADADELTA: an adaptive learning rate method. *arXiv preprint arXiv:1212.5701*, 2012.